Strong interaction between a two-level atom and the whispering-gallery modes of a dielectric microsphere: Quantum-mechanical consideration

V. V. Klimov*
P. N. Lebedev Physical Institute, Russian Academy of Sciences, 53 Lenin Prospect, Moscow 117924, Russia

M. Ducloy
Laboratoire de Physique des Lasers, URA CNRS 282, Université Paris–Nord, Institut Galilee, Avenue J.-B. Clement, F93430 Villetaneuse, France

V. S. Letokhov
Institute of Spectroscopy, Russian Academy of Sciences, Troitsk 142092, Moscow Region, Russia and Ecole Normale Superieure, 24 rue Lhomond, 75231 Paris Cedex 05, France

(Received 15 July 1998)

The interaction is considered between a two-level atom and the continuum of electric field modes falling within the profile of one of the resonance modes of a dielectric microsphere (a whispering gallery mode). Subject to minimal assumptions, simple equations are obtained on first principles, which describe the spectral properties of the one-photon continuum and the relaxation processes occurring therein. If the initial state of the atom is excited, a doublet structure is formed in the emitted photon spectrum, provided that the interaction is strong enough. If it is the microsphere that is excited at the initial instant, the excited photon spectrum depends substantially on the excitation method used. When excitation is optimal, the atom is effectively excited, and a Rabi-doublet is then formed in the fluorescence spectrum. When the excitation conditions are other than optimal, the spectrum becomes of triplet character, and when the deviation from the optimal excitation conditions is strong enough, the atom practically fails to get excited, and the fluorescence spectrum is of singlet type. A considerable part of the results obtained is of a general nature and can easily be applied to other cases of strong interaction between atoms and resonators. [S1050-2947(99)05103-3]

PACS number(s): 42.55.Sa, 42.50.Ct

I. INTRODUCTION

There are several reasons why the interaction between an atom and a microsphere is of interest. First, the microsphere is a high-quality closed cavity with a low mode density in the optical range [1–3]. That this is true has been experimentally demonstrated using silica microspheres whose quality factor for the whispering gallery modes (WGM) reaches as high a value as 10^{10} [4]. Such a microsphere is essentially a top-quality microcavity for photons: even a single photon produces a field of perceptible strength in the vicinity of its surface (both inside and outside). Second, the atom in the region of increased field strength (inside and outside of the microsphere) can be rather strongly coupled to a resonance mode of the microsphere even at a small number of photons [5], and can even be coupled to the vacuum field (vacuum Rabi splitting [6]). Third, there have been proposed and implemented very interesting applications of such atom plus microsphere couples. Specifically, it becomes possible to effect nondemolition detection of trapped photons and determination of their number (Fock's states) by monitoring the ponderomotive action of the evanescent wave of the microsphere near its surface on the atom, resulting in a change of the phase of the atomic wave function [7,8]. Moreover, the high-quality microsphere is a microlaser with a very low lasing threshold [9] and an interesting object for QED experiments [10]. The strong atom-microsphere coupling is potentially important for experimental realization of ''controlled-NOT'' gates for quantum computers [11–14].

When considering the problem of interaction between an atom and a dielectric microsphere, it is convenient to treat two cases: the case of weak nonresonance interaction and that of strong resonance interaction. The case of weak interaction occurs when the atom is far away from the surface of the microsphere or when the atomic transition frequency is far from the resonance frequencies of the microsphere. In that case, the perturbation theory is applicable, and the characteristics of the system atom plus microsphere plus electromagnetic field is only quantitatively different from those in the case where the atom and the microsphere are infinitely far from each other. This case was analyzed in detail in a number of works [15–18].

The case of strong interaction occurs when the atom comes close to the microsphere or when the atomic transition frequency coincides with a resonance mode of the microsphere. In that case, the situation changes qualitatively, and in particular, there becomes possible an efficient absorption by the microsphere of a photon emitted by the atom and vice versa [19–21].

The interaction between a classical oscillator and classical electromagnetic field in the presence of a dielectric microsphere was examined in [22], where the vacuum Rabi splitting of the emission frequency of the atom located outside the microsphere was analyzed in the strong resonance interaction approximation.

With the problem in the classical formulation treated, the need arises in its consideration from the standpoint of quan-

*Electronic address: klimov@rim.phys.msu.su

tum mechanics. The point is that one might expect, because of the smallness of the number of quanta (photons) in the systems, a substantial deviation of the observable characteristics of the system from the classical ones. The solution of the quantum-mechanical problem proves more difficult than that of its classical counterpart, which in the final analysis reduces to the solution of a complex transcendental equation. In the quantum-mechanical case, the problem formulation itself poses considerable difficulties because of the interaction of the atom with a great number (continuum) of electromagnetic modes modified by the presence of the microsphere.

From the quantum-mechanical point of view, the spontaneous emission of an atom in a one-dimensional cavity similar to the Fabry-Pérot type was analyzed in [23]. The quantum-mechanical treatment of the resonance interaction between an atom and a dielectric microsphere was started in our work reported in [24], where we suggested on the basis of not very rigorous considerations an approach to the determination and calculation of the so-called vacuum electric field and the finding on its basis of the vacuum splitting of the levels of the system atom plus dielectric microsphere.

In the present work (see also [25]), this problem is analyzed more rigorously, and the vacuum field emerges as a result of rigorous calculations.

The structure of the rest of the paper is as follows. Section II describes the quantization of an electromagnetic field in the presence of a dielectric microsphere. Section III considers the dynamic properties of the one-photon continuum, which is a subspace of states corresponding to a single photon in a quantized mode (or in the form of the energy of the excited atom). The spectrum of the Hamiltonian of the one-photon continuum is found here, and it is demonstrated that two discrete components are formed in it, which are responsible for the vacuum Rabi splitting. The formation dynamics of the singlet, doublet, and triplet photon spectrum are also examined in this section for various methods of excitation of the system atom plus microsphere. In Sec. IV and V, the results obtained are used to find explicit expressions for the vacuum field and vacuum Rabi frequency for various orientations and positions of the atom. Section VI presents the results of numerical calculations for various problem parameters.

II. QUANTIZATION OF ELECTROMAGNETIC FIELD IN THE PRESENCE OF A DIELECTRIC MICROSPHERE

By and large the quantization procedure for electromagnetic field in spherical geometry is well known [26], but a special approach is required in each particular case. In our problem, the quantization volume may be taken in the form of an ideally conducting sphere of finite but large radius $\Lambda \to \infty$ (the geometry of the problem is shown in Fig. 1). The final results will be independent of Λ. The expansion of electromagnetic field and its vector potential over the complete set of eigenfunctions of the classical problem may be represented in the form [26]

$$\hat{\mathbf{E}} = \sum_s \frac{a_s \mathbf{e}(s,\mathbf{r}) - a_s^\dagger \mathbf{e}^*(s,\mathbf{r})}{i\sqrt{2}},$$

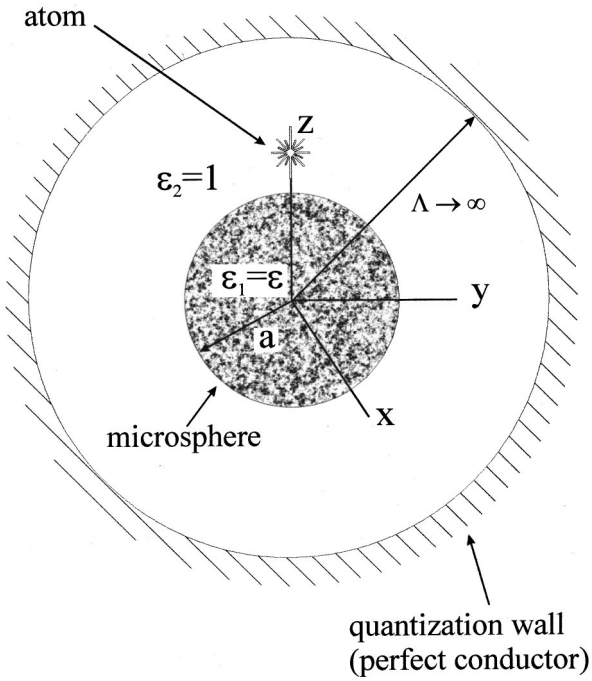

FIG. 1. Geometry of the quantum-mechanical problem of the interaction between a two-level atom and a microsphere.

$$\hat{\mathbf{B}} = \sum_s \frac{a_s \mathbf{b}(s,\mathbf{r}) + a_s^\dagger \mathbf{b}^*(s,\mathbf{r})}{\sqrt{2}}, \tag{2.1}$$

$$\hat{\mathbf{A}} = -\sum_s \frac{c}{\omega_s} \frac{a_s \mathbf{e}(s,\mathbf{r}) + a_s^\dagger \mathbf{e}^*(s,\mathbf{r})}{\sqrt{2}}.$$

The eigenfunctions $\mathbf{b}(s,\mathbf{r}), \mathbf{e}(s,\mathbf{r})$ obey a set of equations:

$$\nabla \times \mathbf{e}(s,\mathbf{r}) = i \frac{\omega_s}{c} \mathbf{b}(s,\mathbf{r}),$$

$$\nabla \times \mathbf{b}(s,\mathbf{r}) = \begin{cases} -i \dfrac{\omega_s}{c} \varepsilon \mathbf{e}(s,\mathbf{r}), & r < a, \\ -i \dfrac{\omega_s}{c} \mathbf{e}(s,\mathbf{r}), & r > a, \end{cases} \tag{2.2}$$

with an appropriate boundary condition at $r = \Lambda$.

Here a_s and $a_s^\dagger$ are the respective photon annihilation and creation coefficients in the corresponding modes with ordinary communication relations and ω_s are the frequencies of these modes.

In the case of electric dipole transitions, it is both transverse magnetic (TM) and transverse electric (TE) modes that can be excited, and where the transition dipole moment is radially oriented, it is only the TM modes that can get excited. It is not very difficult to obtain expressions for the electric field strength $\mathbf{e}(s,\mathbf{r})$ of the sth mode in terms of spherical harmonics (Y_{nm}) and spherical Bessel and Hankel functions (j,h) [27]:

$$\mathbf{e}_{\mathrm{TM}}(n,m,\nu)=\begin{cases} -\dfrac{1}{k\varepsilon}\nabla\times\{[\beta_{\mathrm{TM},n}j_n(k_1r)]\hat{\mathbf{L}}Y_{nm}(\vartheta,\varphi)\}, & r<a, \\ -\dfrac{1}{k}\nabla\times\{[\alpha^{(1)}_{\mathrm{TM},n}h^{(1)}_n(kr)+\alpha^{(2)}_{\mathrm{TM},n}h^{(2)}_n(kr)]\hat{\mathbf{L}}Y_{nm}(\vartheta,\varphi)\}, & r>a \end{cases} \tag{2.3}$$

in the case transverse magnetic modes and

$$\mathbf{e}_{\mathrm{TE}}(n,m,\nu)=\begin{cases} [\beta_{\mathrm{TE},n}j_n(k_1r)]\hat{\mathbf{L}}Y_{nm}(\vartheta,\varphi), & r<a, \\ [\alpha^{(1)}_{\mathrm{TE},n}h^{(1)}_n(kr)+\alpha^{(2)}_{\mathrm{TE},n}h^{(2)}_n(kr)]\hat{\mathbf{L}}Y_{nm}(\vartheta,\varphi), & r>a \end{cases} \tag{2.4}$$

in the case of transverse electric modes. Here n is the orbital quantum number, m is the azimuthal quantum number, ν is the radial quantum number, $k=\omega_s/c$; $k_1=\sqrt{\varepsilon}(\omega_s/c)$ are the wave vectors outside and inside the sphere, respectively, $\mathbf{L}=-i\mathbf{r}\times\boldsymbol{\nabla}$ is the orbital momentum operator, and a is the radius of the microsphere. The quantum number set (n,m,ν) forms the vector index $s=(n,m,\nu)$ used above.

The coefficients α_n and β_n are found in the usual way such that the tangential field components at the microsphere boundary are continuous and the wave functions in the sphere of radius Λ are normalized to a single photon in a quantized mode:

$$\frac{\alpha^{(1)}_{\mathrm{TM}}}{\alpha^{(2)}_{\mathrm{TM}}}=1-2q_n;$$

$$\frac{\beta_{\mathrm{TM}}}{\alpha^{(2)}_{\mathrm{TM}}}=\frac{2i\varepsilon q_n}{ka[\varepsilon(z_2j_n(z_2))'j_n(z_1)-(z_1j_n(z_1))'j_n(z_2)]}, \tag{2.5}$$

$$\frac{\alpha^{(1)}_{\mathrm{TE}}}{\alpha^{(2)}_{\mathrm{TE}}}=1-2p_n;$$

$$\frac{\beta_{\mathrm{TE}}}{\alpha^{(2)}_{\mathrm{TE}}}=\frac{2ip_n}{ka[(z_2j_n(z_2))'j_n(z_1)-(z_1j_n(z_1))'j_n(z_2)]}, \tag{2.6}$$

$$q_n=\frac{\left[\varepsilon\dfrac{d}{dz_2}[z_2j_n(z_2)]j_n(z_1)-\dfrac{d}{dz_1}[z_1j_n(z_1)]j_n(z_2)\right]}{\left[\varepsilon\dfrac{d}{dz_2}[z_2h^{(1)}_n(z_2)]j_n(z_1)-\dfrac{d}{dz_1}[z_1j_n(z_1)]h^{(1)}_n(z_2)\right]}, \tag{2.7}$$

$$p_n=\frac{\left[\dfrac{d}{dz_2}[z_2j_n(z_2)]j_n(z_1)-\dfrac{d}{dz_1}[z_1j_n(z_1)]j_n(z_2)\right]}{\left[\dfrac{d}{dz_2}[z_2h^{(1)}_n(z_2)]j_n(z_1)-\dfrac{d}{dz_1}[z_1j_n(z_1)]h^{(1)}_n(z_2)\right]}, \tag{2.8}$$

$$|\alpha^{(1)}_{\mathrm{TE},n}|^2=|\alpha^{(2)}_{\mathrm{TE},n}|^2=|\alpha^{(1)}_{\mathrm{TM},n}|^2=|\alpha^{(2)}_{\mathrm{TM},n}|^2=\frac{2\pi\hbar c}{\Lambda}\frac{k^3}{n(n+1)}. \tag{2.9}$$

Here q_n and p_n are the Mie reflection coefficients [28], $z_1=k_1a$, $z_2=ka$, and ε is the dielectric constant of the microsphere. Note that with the wave functions normalized, the contribution from the region inside the dielectric microsphere is negligibly small in comparison with that from the region with $r\sim\Lambda$.

To study the interaction between an atomic oscillator and the continuum of electromagnetic modes modified by the presence of a dielectric microsphere, it is also necessary to know the density of final states. The requirement that the tangential electric field components of the TM modes should vanish on the inside surface of the quantization sphere leads to the transcendental equation

$$\left.\frac{d}{dr}(rZ)\right|_{r=\Lambda}=0, \tag{2.10}$$

$$Z=\left[\alpha^{(1)}_{\mathrm{TM},n}h^{(1)}_n\left(\frac{\omega_s}{c}r\right)+\alpha^{(2)}_{\mathrm{TM},n}h^{(2)}_n\left(\frac{\omega_s}{c}r\right)\right],$$

which has the asymptotic solutions

$$\omega_s=\left(\nu+\frac{n+1}{2}\right)\frac{\pi c}{\Lambda}+\cdots, \tag{2.11}$$

where ν is the radial quantum number. Hence it follows that the density of the final states will be defined by the simple expression

$$\rho(\omega)=\frac{d\nu}{d(\hbar\omega_s)}=\frac{\Lambda}{\pi\hbar c}. \tag{2.12}$$

In the case of TE modes, we have the same density of states. Note the density of the final states is independent of the presence of the microsphere ($\Lambda\to\infty$). It is in agreement with Courant's theorem [29].

The discussion up until now has been concerned with arbitrary quantized modes with equidistant frequencies (2.11). But if the resonance conditions are satisfied, there arise whispering gallery modes [1,30,31]. The behavior of the energy of interaction between the atom and the quantized modes [see Eq. (3.8)] falling within the profile of a whispering gallery mode is qualitatively illustrated in Fig. 2.

From the physical standpoint, the development of a whispering gallery mode is associated with the effect of total

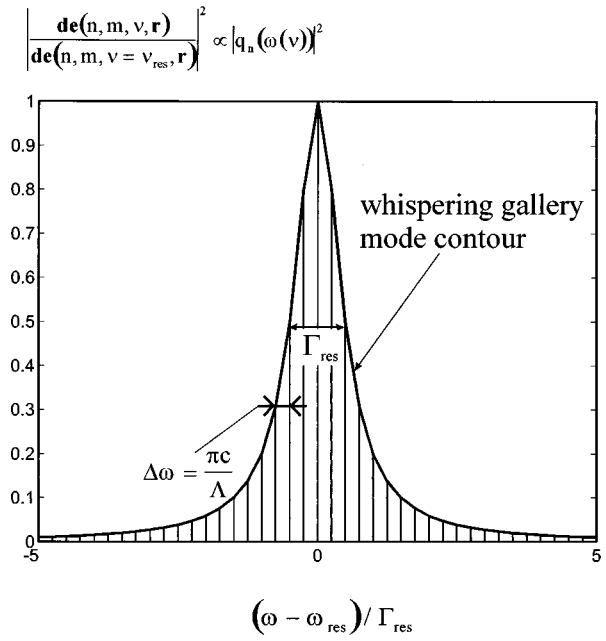

FIG. 2. Illustrating the resonance enhancement of the energy of interaction between an atom and quantized modes [see Eq. (3.8)] falling within the profile of a whispering gallery mode.

internal reflection from the surface of the microsphere, and the frequency of the mode is approximately defined by the Bohr quantization equation

$$2\pi a = N\lambda, \tag{2.13}$$

where λ is the wavelength in the dielectric microsphere.

From the formal standpoint, a whispering gallery mode arises when a pole appears in the Mie reflection coefficients (2.7) and (2.8), for it is only in this case that total internal reflection takes place.

The equations defining the position of resonances may be obtained from Eqs. (2.7) and (2.8):

$$\frac{[J_{n+1/2}(z_1)]'}{J_{n+1/2}(z_1)} = \frac{1}{2z_2}(\sqrt{\varepsilon} - \sqrt{1/\varepsilon}) + \sqrt{\varepsilon}\frac{[H^{(1)}_{n+1/2}(z_2)]'}{H^{(1)}_{n+1/2}(z_2)} \quad \text{(TM case)}, \tag{2.14}$$

$$\frac{[J_{n+1/2}(z_1)]'}{J_{n+1/2}(z_1)} = \left(\frac{1}{\varepsilon}\right)^{1/2}\frac{[H^{(1)}_{n+1/2}(z_2)]'}{H^{(1)}_{n+1/2}(z_2)} \quad \text{(TE case)}, \tag{2.15}$$

where $z_1 = k_1 a$ and $z_2 = ka$.

In the case of whispering gallery modes, a whole number of waves are present along the circumference, i.e., $z_1 \approx n$, $z_2 \approx n/\sqrt{\varepsilon}$. Using this fact, Eqs. (2.14) and (2.15) can be simplified by means of the Debye asymptotic expansions for the Hankel functions and asymptotic expansions in the transitional region for the Bessel functions [27]. As a result, instead of Eqs. (2.14) and (2.15), we get

$$\frac{\mathrm{Ai}'(-2^{1/3}t)}{\mathrm{Ai}(-2^{1/3}t)} = \left(\frac{\nu}{2}\right)^{1/3}\sqrt{\varepsilon}\,\mathrm{sh}\,\alpha(1 - ie^{-2\nu(\alpha - \mathrm{th}\,\alpha)}) \quad \text{(TM case)}, \tag{2.16}$$

$$\frac{\mathrm{Ai}'(-2^{1/3}t)}{\mathrm{Ai}(-2^{1/3}t)} = \left(\frac{\nu}{2}\right)^{1/3}\left(\frac{1}{\varepsilon}\right)^{1/2}\mathrm{sh}\,\alpha(1 - ie^{-2\nu(\alpha - \mathrm{th}\,\alpha)}) \quad \text{(TE case)}. \tag{2.17}$$

Here $\nu = n + 1/2$, $t = (z_1 - \nu)/\nu^{1/3}$, $\mathrm{ch}\,\alpha = \sqrt{\varepsilon}(\nu/z_1)$, and Ai is the Airy function [27].

In the case of large $n(\nu)$, these equations can be solved by iteration with respect to t. As a result, the expressions for the resonant frequencies assume the form [32]

$$\omega_{\mathrm{res}} = \frac{c}{a\sqrt{\varepsilon}}\left(j_{n+1/2} - \frac{1}{\varepsilon}\sqrt{\frac{\varepsilon}{\varepsilon - 1}}\right) \quad \text{(TM case)}, \tag{2.18}$$

$$\omega_{\mathrm{res}} = \frac{c}{a\sqrt{\varepsilon}}\left(j_{n+1/2} - \sqrt{\frac{\varepsilon}{\varepsilon - 1}}\right) \quad \text{(TE case)}, \tag{2.19}$$

where $j_{n+1/2}$ is one of the roots of the Bessel function $J_{n+1/2}$.

When using in Eq. (2.18) or (2.19) the first nontrivial root, there develops a whispering gallery mode having no zeros inside the microsphere; when using the second root, the first zero appears inside the microsphere, and so on. In this connection, whispering gallery modes can conveniently be classified on the basis of three numbers [3,31]: the number of zeros in the radial direction inside the microsphere, the order of the spherical Bessel function, and the azimuthal quantum number. Figures 3 and 4 show the Mie reflection coefficients as a function of the parameter ka. The modes without zeros in the radial direction inside the microsphere are clearly seen (left-hand row).

To estimate the radiative width of the principal resonance line, use can be made of the following formula obtained by iteration from Eqs. (2.16) and (2.17) [32]:

$$\frac{\Gamma_{\mathrm{res}}}{\omega_{\mathrm{res}}} = \frac{1}{Q_{\mathrm{TM}}} \approx \frac{2}{j_{n+1/2}}\frac{1}{\varepsilon}\left(\frac{\varepsilon}{\varepsilon - 1}\right)^{1/2} e^{-2T_{\mathrm{TM}}},$$
$$T_{\mathrm{TM}} = \nu\left(\mathrm{arch}\sqrt{\varepsilon} - \sqrt{1 - \frac{1}{\varepsilon^{1/2}}}\right) - t_0\nu^{1/3}\sqrt{1 - \frac{1}{\varepsilon}} + \frac{1}{\varepsilon} + \cdots \tag{2.20}$$

for TM resonances and the formula

$$\frac{\Gamma_{\mathrm{res}}}{\omega_{\mathrm{res}}} = \frac{1}{Q_{\mathrm{TE}}} \approx \frac{2}{j_{n+1/2}}\left(\frac{\varepsilon}{\varepsilon - 1}\right)^{1/2} e^{-2T_{\mathrm{TE}}},$$
$$T_{\mathrm{TE}} = \nu\left[\mathrm{arch}\sqrt{\varepsilon} - \left(1 - \frac{1}{\varepsilon}\right)^{1/2}\right] - t_0\nu^{1/3}\left(1 - \frac{1}{\varepsilon}\right)^{1/2} + 1 + \cdots \tag{2.21}$$

for TE resonances. In formulas (2.20) and (2.21), $\nu = n + \frac{1}{2}$, $t_0 = (j_{n+1/2} - \nu)/\nu^{1/3}$. For sufficiently large microspheres

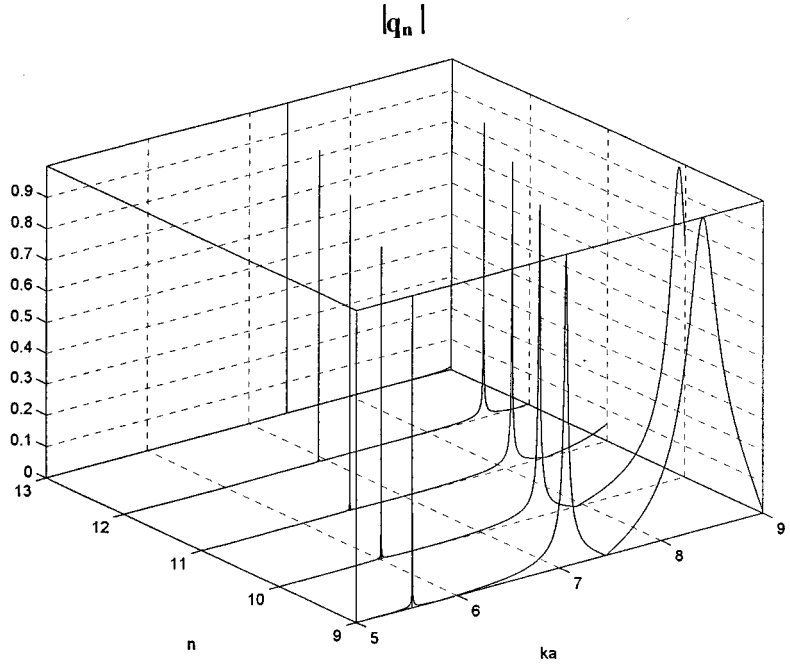

FIG. 3. Positions of the TM whispering gallery modes (relationship between the magnitude of the reflection coefficients q_n of the TM waves and the radius a of the microsphere with $\varepsilon=6$).

($k_0a>100$), the radiative linewidths (2.20) and (2.21) become negligibly small in comparison with other types of loss (absorption in the material, scattering by surface irregularities, etc.). In the case of small microspheres of interest to us, radiative losses are predominant, and so we will give no consideration for the other types of loss in the further discussion.

In the vicinity of resonance, the Mie reflection coefficients assume the following simple form:

$$q_n \approx -i\frac{\mathrm{Im}(\Omega_{\mathrm{res}})}{\omega-\Omega_{\mathrm{res}}}, \tag{2.22}$$

where Ω_{res} is the complex frequency characterizing the resonance mode: $\Omega_{\mathrm{res}}=\omega_{\mathrm{res}}-i(\Gamma_{\mathrm{res}}/2)$, and Γ_{res} characterizes the width of the resonance mode and the Q factor of the cavity with this mode. Similar expressions are also valid for TE modes:

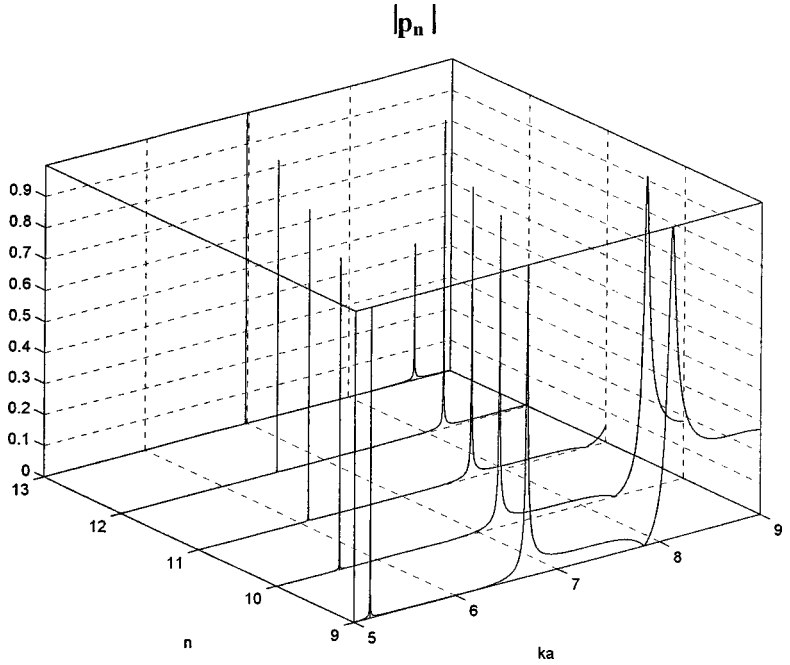

FIG. 4. Positions of the TE whispering gallery modes (relationship between the magnitude of the reflection coefficients p_n of the TE waves and the radius a of the microsphere with $\varepsilon=6$).

$$p_n \approx -i\frac{\mathrm{Im}(\Omega_{\mathrm{res}})}{\omega-\Omega_{\mathrm{res}}}. \tag{2.23}$$

III. ONE-PHOTON CONTINUUM DYNAMICS

A. One-photon continuum Hamiltonian

In the case of resonance interaction between an atom and long-lived electromagnetic field modes in a microsphere (the so-called whispering gallery modes [1,30,31]), which is of interest to us, the effective dipolar atom-field interaction Hamiltonian may be represented in the form [33,34]

$$H=H_A+H_F+H_I, \tag{3.1}$$

where the atomic Hamiltonian H_A, field Hamiltonian H_F, and interaction Hamiltonian H_I for the two-level atom under consideration have the following form:

$$H_A=\hbar\omega_A\begin{pmatrix}1\\0\end{pmatrix},$$

$$H_F=\sum_s \hbar\omega_s a_s^\dagger a_s, \tag{3.2}$$

$$H_I=-\hat{\mathbf{d}}\otimes\hat{\mathbf{E}}.$$

Here $a_s^\dagger$ and a_s are the ordinary creation and annihilation Bose operators for photons with the frequency ω_s in the resonance mode of the microsphere, $\hat{\mathbf{d}}$ is the dipole moment operator given by

$$\hat{\mathbf{d}}=\begin{pmatrix}0 & \mathbf{d}\\ \mathbf{d}^* & 0\end{pmatrix}, \tag{3.3}$$

and the symbol $\otimes$ denotes the direct multiplication of the atomic and photonic states.

Consider the parameters of this Hamiltonian. The magnitude of the dipole transition moment d should be taken equal to that in the absence of interaction. As for the atomic transition frequency ω_A, it seems quite logical that it allows for the shift due to the purely electrostatic interaction with the microsphere [17,18,22,24].

In accordance with Eqs. (2.22) and (2.23), the resonance linewidth is finite, and account should be taken of all the discrete modes $\omega_1,\omega_2,\omega_3,\ldots$ falling within the resonance profile, including the modes that are degenerate as to the azimuthal quantum number (see Fig. 2).

Considering what has been said above, Hamiltonian (3.1) may be represented by a matrix of the form

$$H=\begin{pmatrix}0 & 0 & X & \cdots\\ 0 & H_1 & 0 & \cdots\\ X^* & 0 & H_2 & \cdots\\ \cdots & \cdots & \cdots & \cdots\end{pmatrix}, \tag{3.4}$$

where H_1 is the Hamiltonian corresponding to the one-photon continuum,

$$H_1=\begin{pmatrix}\hbar\omega_A & V_1 & V_2 & V_3\\ V_1^* & \hbar\omega_1 & 0 & 0\\ V_2^* & 0 & \hbar\omega_2 & 0\\ V_3^* & 0 & 0 & \hbar\omega_3\end{pmatrix}, \tag{3.5}$$

H_2 is the Hamiltonian corresponding to the two-photon continuum,

$$H_2=\begin{pmatrix}
\hbar(\omega_A+\omega_1) & 0 & 0 & \sqrt{2}V_1 & 0 & 0 & V_2 & V_3 & 0\\
0 & \hbar(\omega_A+\omega_2) & 0 & 0 & \sqrt{2}V_2 & 0 & V_1 & 0 & V_3\\
0 & 0 & \hbar(\omega_A+\omega_3) & 0 & 0 & \sqrt{2}V_3 & 0 & V_1 & V_2\\
\sqrt{2}V_1^* & 0 & 0 & 2\hbar\omega_1 & 0 & 0 & 0 & 0 & 0\\
0 & \sqrt{2}V_2^* & 0 & 0 & 2\hbar\omega_2 & 0 & 0 & 0 & 0\\
0 & 0 & \sqrt{2}V_3^* & 0 & 0 & 2\hbar\omega_3 & 0 & 0 & 0\\
V_2^* & V_1^* & 0 & 0 & 0 & 0 & \hbar(\omega_1+\omega_2) & 0 & 0\\
V_3^* & 0 & V_1^* & 0 & 0 & 0 & 0 & \hbar(\omega_1+\omega_3) & 0\\
0 & V_3^* & V_2^* & 0 & 0 & 0 & 0 & 0 & \hbar(\omega_2+\omega_3)
\end{pmatrix}, \tag{3.6}$$

and the X terms describe transitions involving two-unit changes in the number of photons,

$$X=(\tilde{V}_1\ \ \tilde{V}_2\ \ \tilde{V}_3\ \ 0\ \ 0\ \ 0\ \ 0\ \ 0\ \ 0). \tag{3.7}$$

In writing expressions (3.5)–(3.7), we adopted for clarity that the atomic oscillator interacts with three quantized modes ω_1, ω_2, and ω_3. The generalization to a greater number of modes (the continuum of modes in the limit) is not very difficult to make. The state vector of our system has the following structure:

ground state

excited atom (ω_A)
one photon (ω_1)
one photon (ω_2) } one-photon continuum
one photon(ω_3)
...

excited atom (ω_A)+one photon (ω_1)
excited atom (ω_A)+one photon (ω_2)
...
two photons (ω_1)
two photons (ω_2) } two-photon continuum
two photons(ω_3)
...

etc.

Note that only two-photon states are numbered as follows: the states with two photons in the same state $2\omega_1,2\omega_2,2\omega_3,\ldots$ come first, and next come the states with an energy of $\omega_i+\omega_j$, $i<j$. The interaction matrix elements $V_{j,m},\tilde{V}_{j,m}$ have the usual form

$$V_{j,m}=V_m(\omega_j)=-\frac{\mathbf{de}(n,m,\nu_j,\mathbf{r})}{i\sqrt{2}},$$

$$\tilde{V}_{j,m}=-\frac{\mathbf{d}^*\mathbf{e}(n,m,\nu_j,\mathbf{r})}{i\sqrt{2}}, \tag{3.8}$$

where $\mathbf{e}$ is the electric field strength of the quantized mode, given by Eqs. (2.3) and (2.4).

In the rotating-wave approximation, the matrix X can be disregarded, and the interaction Hamiltonian for a two-level atom and a continuum of modes will then assume the form of the block-diagonal matrix

$$H=\begin{pmatrix} 0 & 0 & 0 & \cdots \\ 0 & H_1 & 0 & \cdots \\ 0 & 0 & H_2 & \cdots \\ \cdots & \cdots & \cdots & \cdots \end{pmatrix}, \tag{3.9}$$

wherein the one-photon and two-photon continua with correspondent atomic states do not interact and one can consider them separately.

In this work we consider a one-photon continuum, described by Hamiltonian (3.5). Hamiltonian (3.5) was considered in general form in a number of papers (for example, [19,34,35]). Expressions for the line profile were found in [36,37] with the assumption of frequency independence of the matrix elements V_{im}. In the present work, we will analyze the dynamics of the system with Hamiltonian (3.5) subject to the condition that the coefficients V_{im} depend on frequency in a resonance fashion. To find the spectrum of this Hamiltonian is a difficult task, but if the linewidth of the whispering gallery mode is small (the smallness criterion will be evident below), the energies of all the photons in Hamiltonian (3.5) can be taken to be equal to the photon energy in the case of resonance: $\omega_i=\omega_{\rm res}$. In that case, of course, the nondiagonal elements V_i describing the resonance interaction will change greatly as a function of frequency.

As a result of the above approximation, the interaction Hamiltonian for an atom and one-photon continuum will assume the form

$$H_1=\begin{pmatrix} \hbar\omega_A & V_1 & V_2 & V_3 \\ V_1^* & \hbar\omega_{\rm res} & 0 & 0 \\ V_2^* & 0 & \hbar\omega_{\rm res} & 0 \\ V_3^* & 0 & 0 & \hbar\omega_{\rm res} \end{pmatrix}. \tag{3.10}$$

It is not very difficult to verify that the spectrum of such a Hamiltonian has $n-1$ degenerate eigenvalues $\omega_{\rm res}$ (n is the number of quantized modes) and the two nontrivial eigenvalues

$$\hbar\omega_{\pm}=\hbar\left(\frac{\omega_{\rm res}+\omega_A}{2}\pm\tfrac{1}{2}\sqrt{(\omega_{\rm res}-\omega_A)^2+4\Omega_{\rm Rabi}^2}\right) \tag{3.11}$$

which point to the emergence of two discrete components instead of one at $\omega_{\rm res}=\omega_A$. In Eq. (3.11), the vacuum Rabi frequency is defined by the expression

$$\hbar^2\Omega_{\rm Rabi}^2=\sum_{i,m}|V_{i,m}|^2=\sum_m\int d(\hbar\omega)\rho(\omega)|V_m(\omega)|^2 \tag{3.12}$$

which is exact despite approximation (3.10).

Note that a similar expression for the vacuum Rabi frequency was obtained in [35] on the basis of another approach. Since we are considering here the resonance interaction, then, according to Eqs. (2.22) and (2.23), the relation

$$\rho(\omega_i)|V_{im}|^2\propto\frac{1}{|\omega_i-\Omega_{\rm res}|^2} \tag{3.13}$$

holds true, and consequently one can easily get from expression (3.12) the general relation

$$\rho(\omega_i)\sum_m|V_m(\omega_i)|^2=\frac{\Gamma_{\rm res}/2}{(\omega_i-\omega_{\rm res})^2+\Gamma_{\rm res}^2/4}\frac{\hbar}{\pi}\Omega_{\rm Rabi}^2. \tag{3.14}$$

Where the variation of the quantized mode frequencies within the limits of resonance cannot be neglected, the degeneration in Eq. (3.10) is removed. Nevertheless, if the Rabi

frequency given by expression (3.12) exceeds the linewidth of the whispering gallery mode, the approximate Hamiltonian will correctly define the vacuum Rabi splitting.

Substituting expression (3.8) into Eq. (3.12), one can easily obtain the following expression for the Rabi frequency in terms of the electric field strength of the mode:

$$\hbar^2|\Omega_{\mathrm{Rabi}}(\mathbf{r})|^2=\tfrac{1}{2}\sum_j\ \sum_m\ |\mathbf{de}(n,m,\nu_j,\mathbf{r})|^2. \quad (3.15)$$

Note that the above expression for the Rabi frequency agrees with the following Rabi frequency *definition* presented in [21,24] without proof:

$$\hbar^2|\Omega_{\mathrm{Rabi}}(\mathbf{r})|^2=\underset{\mathrm{def}}{\langle \mathrm{vac}|(\hat{\mathbf{d}}\hat{\mathbf{E}})^2|\mathrm{vac}\rangle}$$

$$=\tfrac{1}{2}\sum_i\ \sum_m\ |\mathbf{de}(n,m,\nu_i,\mathbf{r})|^2. \quad (3.15a)$$

With Rabi frequency (3.15) found, the estimation of the spectrum of Hamiltonian (3.5) can be considered to be completed. However, the presence of discrete components in the spectrum is in no way a sufficient condition for the development of a doublet structure in the emitted photon spectrum.

B. Properties of the one-photon continuum in the case where the atom is excited

To describe the doublet structure of the emitted photon spectrum, one should analyze the dynamics of the system described by the Schrödinger equation with Hamiltonian (3.5). This problem was considered in the general form in [19], but the approximations and assumptions made in this work require further investigation.

The Schrödinger equations for the coefficient of expansion in terms of eigenfunctions of the free Hamiltonian of the one-photon continuum (probability amplitudes) have the form

$$i\frac{\partial\psi_A(t)}{\partial t}=\omega_A\psi_A(t)+\sum_{j,m}\frac{V_{j,m}}{\hbar}\psi_{j,m}(t),$$

$$i\frac{\partial\psi_{j,m}(t)}{\partial t}=\omega_j\psi_{j,m}(t)+\frac{V^*_{j,m}}{\hbar}\psi_A(t),\quad m=0,\pm1,...\pm n; \quad (3.16)$$

$$j=1,2,\ldots.$$

Here $\psi_A,\psi_{i,m}$ are the probability amplitudes to find an atom or quantized mode with radial quantum number ν_i and azimuthal quantum number m in an excited state, respectively.

Taking Fourier transform (3.16) with due regard for the fact that the atom was in an excited state at the initial instant of time, we get the system

$$(\omega-\omega_A)\psi_A(\omega)=\sum_{j,m}\frac{V_{j,m}}{\hbar}\psi_{j,m}(\omega)+i2,$$

$$(\omega-\omega_j)\psi_{j,m}(\omega)=\frac{V^*_{j,m}}{\hbar}\psi_A(\omega),\quad m=0,\pm1,...\pm n; \quad (3.17)$$

$$j=1,2,\ldots.$$

Excluding from expression (3.17) the photon components $\psi_{j,m}(\omega)$, we obtain the following expression for the Fourier component $\psi_A(\omega)$:

$$\psi_A(\omega)=\frac{-i}{\omega-\omega_A-\Sigma_A(\omega)}, \quad (3.18)$$

where the mass operator $\Sigma_A(\omega)$ is defined by the expression

$$\Sigma_A(\omega)=-\frac{1}{\hbar}\sum_m\ \int\frac{d\omega'\rho(\omega')|V_m(\omega')|^2}{\omega'-\omega-i0^+}. \quad (3.19)$$

Substituting expression (3.14) into Eq. (3.19) and calculating the resultant integral, we get the following relation for the mass operator:

$$\Sigma_A(\omega)=\frac{\Omega^2_{\mathrm{Rabi}}}{\omega-\Omega_{\mathrm{res}}}. \quad (3.20)$$

Accordingly, for the Fourier component of the atomic wave function, we have the following rather simple expression:

$$\psi_A(\omega)=\frac{i(\omega-\Omega_{\mathrm{res}})}{(\omega-\omega_A)(\omega-\Omega_{\mathrm{res}})-\Omega^2_{\mathrm{Rabi}}}. \quad (3.21)$$

Going over into the time domain, one can easily find the amplitude of the probability that the atom will be in an excited state:

$$\psi_A(t)=\frac{1}{\omega_+-\omega_-}\{e^{-i\omega_+t}(\omega_+-\Omega_{\mathrm{res}})-e^{-i\omega_-t}(\omega_--\Omega_{\mathrm{res}})\}, \quad (3.22)$$

where ω_+,ω_- are the solutions of the dispersion equation

$$(\omega-\omega_A)(\omega-\Omega_{\mathrm{res}})-\Omega^2_{\mathrm{Rabi}}=D(\omega)=0, \quad (3.23)$$

$$\omega_\pm=\frac{(\omega_A+\Omega_{\mathrm{res}})\pm\sqrt{(\omega_A-\Omega_{\mathrm{res}})^2+4\Omega^2_{\mathrm{Rabi}}}}{2}. \quad (3.24)$$

Both dispersion equation (3.23) and its solution (3.24) largely coincide with the dispersion equation and solution of the classical problem on the interaction between the classical oscillator and classical electromagnetic field [22]. Note that in contrast to spectrum estimate (3.11), dispersion equation solution (3.24) contains imaginary parts which are responsible for the relaxation processes and can be obtained by the substitution $\omega_{\mathrm{res}}\rightarrow\Omega_{\mathrm{res}}$.

Now that the solution for the amplitude of the probability of the atom in an excited state is known, it is not very difficult to find the expression for the Fourier component of the amplitude of the probability that the photon will be in the ith mode:

$$\psi_{i,m}(\omega)=\frac{i(\omega-\Omega_{\mathrm{res}})}{(\omega-\omega_A)(\omega-\Omega_{\mathrm{res}})-\Omega^2_{\mathrm{Rabi}}}\frac{V^*_{i,m}}{\hbar(\omega-\omega_i+i0^+)}. \quad (3.25)$$

For the time dependence of this amplitude, we have

$$\psi_{i,m}(t)=\frac{V_{i,m}^{*}}{\hbar}\left[\begin{array}{l}\dfrac{1}{\omega_+-\omega_-}\left\{e^{-i\omega_+t}\dfrac{(\omega_+-\Omega_{\rm res})}{(\omega_+-\omega_i)}-e^{-i\omega_-t}\dfrac{(\omega_--\Omega_{\rm res})}{(\omega_+-\omega_i)}\right\}\\ +e^{-i\omega_+t}\dfrac{(\omega_i-\Omega_{\rm res})}{(\omega_i-\omega_A)(\omega_i-\Omega_{\rm res})-\Omega_{\rm Rabi}^2}\end{array}\right]. \tag{3.26}$$

When $t\to\infty$, the first two exponentials in Eq. (3.26) go to zero, and the spectral distribution of the emitted photons assumes the form

$$\frac{dP(\omega)}{d(\hbar\omega)}=\sum_m |\psi_{i,m}(t=\infty)|^2\rho(\omega_i)=\frac{\Gamma_{\rm res}}{(2\pi\hbar)}\frac{\Omega_{\rm Rabi}^2}{|D(\omega)|^2}$$
$$=\frac{\Omega_{\rm Rabi}^2\Gamma_{\rm res}/(2\pi\hbar)}{[(\omega_i-\omega_A)(\omega_i-\omega_{\rm res})-\Omega_{\rm Rabi}^2]^2+(\omega_i-\omega_A)^2\Gamma_{\rm res}^2/4}, \tag{3.27}$$

where $D(\omega)$ is defined in Eq. (3.23).

In the case of resonance, i.e., in the case where the atomic transition frequency coincides with the whispering gallery mode frequency ($\omega_A=\omega_{\rm res}$), one can easily find from Eq. (3.27) that the position of the doublet lines is defined by the expression

$$\omega=\omega_A\pm\sqrt{\Omega_{\rm Rabi}^2-\Gamma_{\rm res}^2/8}, \tag{3.28}$$

from which it follows that the Rabi splitting is only possible if

$$\Omega_{\rm Rabi}>\frac{\Gamma_{\rm res}}{2\sqrt{2}}. \tag{3.29}$$

The width of the doublet lines in that case is

$$\frac{\Gamma_{\rm doublet}^2}{4}=\frac{\Gamma_{\rm res}^2}{16}\frac{(\Omega_{\rm Rabi}^2-\Gamma_{\rm res}^2/16)}{(\Omega_{\rm Rabi}^2-\Gamma_{\rm res}^2/8)}. \tag{3.30}$$

If the condition (3.29) is not fulfilled, there occurs the Weisskopf-Wigner exponential decay regime [38], and the spontaneous emission spectrum is a singlet with the linewidth

$$\frac{\Gamma_{\rm singlet}^2}{4}=\frac{4\Omega_{\rm Rabi}^4}{\Gamma_{\rm res}^2-8\Omega_{\rm Rabi}^2}. \tag{3.31}$$

Naturally, expression (3.31) is only valid for a sufficiently strong interaction, i.e., for the case where the Rabi frequency substantially exceeds the atomic linewidth γ_0 in free space.

Expressions (3.21)–(3.31) have been obtained on first principles and are the main result of the present section. With the concrete values of the Rabi frequency $\Omega_{\rm Rabi}$ and resonance frequency $\Omega_{\rm res}$ found, they can be applied to the description of resonance interaction with any cavity. Note that our results considerably refine the results obtained in [19], where the actual cavity was approximated by a singlet providing for the origination of the Rabi frequency and nonresonance absorption in the cavity walls, i.e., use was made of the model non-Hermitian Hamiltonian

$$\tilde{H}_1=\begin{pmatrix}\hbar(\omega_{\rm res}-\delta_c+i\gamma_c) & \hbar\Omega_{\rm Rabi} & 0 & 0 & 0 & \cdots\\ \hbar\Omega_{\rm Rabi} & \hbar\omega_A & 0 & 0 & 0 & \cdots\\ V_1 & 0 & \hbar\omega_1 & 0 & 0 & \cdots\\ V_2 & 0 & 0 & \hbar\omega_2 & 0 & \cdots\\ V_3 & 0 & 0 & 0 & \hbar\omega_3 & \cdots\\ \cdots & \cdots & \cdots & \cdots & \cdots & \cdots\end{pmatrix} \tag{3.32}$$

which allowed simple diagonalization but could not help find concrete Rabi frequency and doublet linewidth values.

C. Properties of the one-photon continuum in the case where the microsphere is excited

In this case, Eqs. (3.16) defining the dynamics of the system atom plus microsphere remain the same. A difference occurs in the formulation of the initial conditions. We will assume that the excitation energy of the microsphere is distributed among the quantized modes as follows:

$$\psi_{j,m}(t=0)=\psi_{0,j,m}, \quad \sum_{j,m}|\psi_{0,j,m}|^2=1. \tag{3.33}$$

In the secondary quantization representation (the Fock representation), this is equivalent to the selection of the initial state in the form

$$|\psi_{\rm photon}(t=0)\rangle=\sum_{j,m}\psi_{0,j,m}|1\rangle_{j,m}, \tag{3.34}$$

where $|1\rangle_{j,m}$ is the one-photon Fock state with the energy $\hbar\omega_j$ and mode structure $\mathbf{e}^{\rm TE}(n,m,\nu_j,\mathbf{r})$ or $\mathbf{e}^{\rm TM}(n,m,\nu_j,\mathbf{r})$, the phase of $\psi_{0,j,m}$ being reckoned with respect to that of $\mathbf{e}^{\rm TE}(n,m,\nu_j,\mathbf{r})$ or $\mathbf{e}^{\rm TM}(n,m,\nu_j,\mathbf{r})$, so that the absolute phase values of the interaction matrix elements appear nowhere.

The mean energy of any state (3.34) is equal to $\hbar\omega_{\rm res}$. To understand the physical meaning of the initial conditions

(3.33) or (3.34), let us consider the mean value of the squared radial component of the electric field operator of the TM mode:

$$S_0(r)=\langle\psi_{\text{photon}}(t=0)|\hat{E}^2_{\text{rad}}(r)|\psi_{\text{photon}}(t=0)\rangle. \quad (3.35)$$

For not too large distances from the microsphere center $[(r/c)\Gamma_{\text{res}}\ll 1]$, it is possible to find from Eq. (3.35) the relationship between the squared electric field strength and initial distribution (3.33):

$$S_0(r)\propto\left(\tfrac{1}{2}\sum_j\left|q(\omega_j)\right|^2+\left|\sum_j q(\omega_j)\psi_{0,j,0}\right|^2\right). \quad (3.36)$$

Here $q(\omega)$ is defined by expression (2.7) or (2.22). One can see from the above expression that if $\psi_{0,j,0}\| q(\omega_j)$, the squared electric field strength (and energy) reaches its maximum value near the microsphere. But if $\psi_{0,j,0}\perp q(\omega_j)$, the squared electric field strength and energy in the vicinity of the microsphere are minimal. Thus, expression (3.33) characterizes the spatial structure of one-photon excitation.

Subject to the above initial conditions, the equations for the Fourier components of the probability amplitudes will assume the form

$$(\omega-\omega_A)\psi_A(\omega)=\sum_{j,m}\frac{V_{j,m}}{\hbar}\psi_{j,m}(\omega),$$
$$(\omega-\omega_j)\psi_{j,m}(\omega)=\frac{V^*_{j,m}}{\hbar}\psi_A(\omega)+i\psi_{0,j,m}, \quad (3.37)$$
$$m=0,\pm 1,\ldots\pm n;\quad j=1,2,\ldots.$$

The solution of system (3.37) is a more difficult problem in comparison with the case of an initially excited atom. The point is that the initial conditions are described, generally speaking, by the arbitrary function $\psi_{0,j,m}$, and depending on its form, the emitted photon spectrum and atomic excitation dynamics can assume different forms. In particular, the doublet structure of the photon spectrum (typical of the case of an initially excited atom) will rather be the exception than the rule. This is due to the fact that when the choice of the excitation form of the microsphere is arbitrary, only part of the excitation energy is transformed into the Rabi doublet, the rest of the energy being reemitted without any change in frequency.

To prove this fact, let us first consider the photon emission spectrum in the case of an arbitrary microsphere excitation line shape. From Eq. (3.37) one can easily find the expression for the fluorescence spectrum at $t\to\infty$:

$$\frac{dP(\omega)}{d(\hbar\omega)}=\rho(\omega)\sum_m\left|\frac{V^*_m(\omega)}{\hbar}\psi_A(\omega)+i\psi_{0,m}(\omega)\right|^2. \quad (3.38)$$

In our case, the matrix elements $V^*_m(\omega)$ have the Lorentzian line shape [see Eq. (3.13)]

$$V_m(\omega)\approx\frac{\alpha_m}{\omega-\Omega_{\text{res}}}. \quad (3.39)$$

Assume that the excitation line shape is also of Lorentzian form:

$$\psi_{0,m}(\omega)=\frac{\beta_m}{\omega-\Omega^*_\psi}. \quad (3.40)$$

Substituting Eqs. (3.39) and (3.40) into Eq. (3.38), we get the following expression for the fluorescence spectrum:

$$\frac{dP(\omega)}{d(\hbar\omega)}=\rho(\omega)\sum_m\left|\frac{\alpha^*_m}{\omega-\Omega^*_{\text{res}}}\frac{\psi_A(\omega)}{\hbar}+i\frac{\beta_m}{\omega-\Omega^*_\psi}\right|^2. \quad (3.41)$$

For the Rabi doublet to form, it is necessary that there are no poles between its components in Eq. (3.41), i.e., there are no pole at $\omega=\Omega_\psi$. One can easily see that it is only possible subject to the following conditions. First, the complex resonance frequency of the excitation line must be equal to that of the microsphere:

$$\Omega_\psi=\Omega_{\text{res}}. \quad (3.42)$$

Second, the spatial distribution of the excitation modes must also agree with that of the atom-field interaction matrix element:

$$\beta_m=i\frac{\alpha^*_m}{\hbar}\psi_A(\Omega^*_{\text{res}})=\frac{\alpha^*_m}{\hbar\Omega_{\text{Rabi}}}. \quad (3.43)$$

If conditions (3.42) and (3.43) are not satisfied, the additional poles will not cancel and the fluorescence spectrum will be of triplet or singlet form.

To obtain concrete analytical results, assume that the initial excitation distribution among the microsphere modes has the form

$$\psi_{0,m}(\omega)=\frac{1}{\hbar\Omega_{\text{Rabi}}}\left(\frac{\Gamma_\psi}{\Gamma_{\text{res}}}\right)^{1/2}\frac{\alpha^*_m}{\omega-\Omega^*_\psi},\quad \Omega_\psi=\psi_\psi-i\frac{\Gamma_\psi}{2},$$
$$\Gamma_\psi>0. \quad (3.44)$$

Excluding from expression (3.37) the photon probability amplitudes, we obtain the following expression for the Fourier component of the atomic probability amplitude:

$$\psi_A(\omega)=+\frac{\Omega_{\text{Rabi}}}{D(\omega)}\frac{\sqrt{\Gamma_{\text{res}}\Gamma_\psi}}{\Omega_{\text{res}}-\Omega^*_\psi}, \quad (3.45)$$

where $D(\omega)$ is defined in Eq. (3.23).

It can be seen from this equation that the probability amplitude of the excited state of the atom is proportional to the factor

$$\frac{\sqrt{\Gamma_{\text{res}}\Gamma_\psi}}{\Omega_{\text{res}}-\Omega^*_\psi}, \quad (3.46)$$

which is a maximum at $\Omega_\psi=\Omega_{\text{res}}$. If this condition is satisfied, the atom gets fully excited by the microsphere and the vacuum Rabi splitting occurs. If condition (3.42) is not satisfied, then, as seen from Eq. (3.46), the atom is excited

incompletely, and a central component appears in the fluorescence spectrum along with the Rabi components, i.e., a triplet is formed.

Next substituting Eq. (3.45) into Eq. (3.38), one can find the fluorescence spectrum:

$$\frac{dP(\omega)}{d(\hbar\omega)}=\frac{\Gamma_\psi}{2\pi\hbar}\left|\frac{\Omega_{\mathrm{Rabi}}^2}{(\omega-\Omega_{\mathrm{res}}^*)D(\omega)}\frac{\Gamma_{\mathrm{res}}}{\Omega_{\mathrm{res}}-\Omega_\psi^*}+i\frac{1}{\omega-\Omega_\psi^*}\right|^2, \tag{3.47}$$

where $D(\omega)$ is defined in Eq. (3.23). Here the triplet structure of the spectrum is explicitly expressed. Note that triplet structure (3.47) bears no relation to Mollow's triplet [39], for in this work we consider the one-photon continuum, while Mollow's spectrum develops at high intensities.

As the width of the excitation line tends to zero, the fluorescence spectrum naturally tends to the δ function,

$$\frac{dP(\omega)}{d(\hbar\omega)}_{\Gamma_\psi\to 0}=\frac{\Gamma_\psi}{2\pi\hbar}\left|\frac{1}{\omega-\Omega_\psi^*}\right|^2\approx\delta(\omega-\omega_\psi). \tag{3.48}$$

In the optimum case given by Eqs. (3.42) and (3.43), the expression for the Fourier component of the excited atom probability amplitude will assume the following form:

$$\psi_A(\omega)=\frac{i\Omega_{\mathrm{Rabi}}}{D(\omega)}, \tag{3.49}$$

where $D(\omega)$ is defined in Eq. (3.23).

In the optimum case, one can easily get from Eq. (3.47) the following expression for the emitted photon spectrum:

$$\frac{dP(\omega)}{d(\hbar\omega)}=\frac{\Gamma_{\mathrm{res}}}{2\pi\hbar}\left|\frac{\omega-\omega_A}{D(\omega)}\right|^2=\frac{(\omega-\omega_A)^2\Gamma_{\mathrm{res}}/(2\pi\hbar)}{[(\omega-\omega_A)(\omega-\omega_{\mathrm{res}})-\Omega_{\mathrm{Rabi}}^2]^2+(\omega-\omega_A)^2\Gamma_{\mathrm{res}}^2/4}, \tag{3.50}$$

which is very close to expression (3.27) for the doublet spectrum of photons emitted in the case of initially excited atom. The essential difference from the case of an initially excited atom is that spectrum (3.47) is always of doublet character, even if interaction weakness condition (3.29) is satisfied, i.e., even in the case of the Weisskopf-Wigner regime [38].

Above we considered the case where excitation is to a greater or lesser extent phase-matched with the atom-field interaction matrix elements. Other cases can also be analyzed within the framework of the present approach. In particular, if we use instead of Eq. (3.44) the initial condition

$$\psi_{0,m}(\omega)=\left(\frac{\Gamma_\psi}{\Gamma_{\mathrm{res}}}\right)^{1/2}\frac{1}{\hbar\Omega_{\mathrm{Rabi}}}\frac{\alpha_m^*}{\omega-\Omega_\psi^*},\quad \Omega_\psi=\omega_\psi+i\frac{\Gamma_\psi}{2},\quad \Gamma_\psi>0 \tag{3.51}$$

(phase antimatching), the Fourier component of the excited atom probability amplitude will be described by the expression

$$\psi_A(\omega)=\frac{\Omega_{\mathrm{Rabi}}}{D(\omega)}\frac{\sqrt{\Gamma_{\mathrm{res}}\Gamma_\psi}}{\omega-\Omega_\psi^*}, \tag{3.52}$$

which explicitly contains three frequencies at a sufficiently high Rabi frequency [see Eq. (3.29)].

In the case of antimatching (3.51), the fluorescence spectrum is given by the following expression ($\omega_A=\omega_{\mathrm{res}}$):

$$\frac{dP(\omega)}{d(\hbar\omega)}=\frac{\Gamma_\psi}{2\pi\hbar}\frac{1}{|\omega-\Omega_\psi|^2}. \tag{3.53}$$

This spectrum is always of singlet type, and as the excitation linewidth tends to zero, it is naturally reduced to δ function (3.48).

The case of uniform distribution of the phase

$$\psi_{0,m}(\omega)=\frac{1}{\hbar\Omega_{\mathrm{Rabi}}}\left(\frac{\Gamma_\psi}{\Gamma_{\mathrm{res}}}\right)^{1/2}\frac{\alpha_m^*}{|\omega-\Omega_\psi^*|},\quad \Omega_\psi=\omega_\psi-i\frac{\Gamma_\psi}{2},\quad \Gamma_\psi>0 \tag{3.54}$$

is an intermediate between cases (3.44) and (3.51) and can also be analyzed within the framework of our approach.

Above we have considered various cases differing in the frequency distribution of the excitation line phase, the relative phase being taken to be actually independent of the azimuthal quantum number m. That is to say, we have assumed a perfect match as to the azimuthal quantum number. Such an approach is completely justified in the case of radial orientation of the atomic dipole moment, for the atom here interacts only with the mode having $m=0$ (in the coordinate system wherein the atom is situated on the polar axis) and the phase problem is altogether absent. In the case of arbitrary orientation of the dipole moment, the atom interacts with the modes having $m=0,\pm 1$, and, generally speaking, it is necessary to make special efforts to ensure coherence as to m [condition (3.43)]. Note that the modes with $m\neq 0,\pm 1$ (in the coordinate system wherein the atom is located on the polar axis) do not interact at all with the atom and manifest themselves in the fluorescence spectrum without any change.

It should be emphasized that the cases of excitation of the microsphere modes considered above are characterized by a certain degree of coherence between various quantized modes. Naturally no splitting takes place in the case of noncoherent excitation of the microsphere (random phase distribution among the quantized modes).

IV. VACUUM FIELD AND RABI FREQUENCY IN THE CASE OF AN ATOM LOCATED OUTSIDE OF THE MICROSPHERE

A. Radial dipole moment orientation

We proceed to the direct calculation of the Rabi frequency. Consider first the case of an atom located outside of the microsphere. In the case where the transition dipole moment element is oriented along the radius of the dielectric microsphere, interaction is only possible with its TM modes and it is then necessary to examine the mean square of the radial electric field component in the TM mode:

$$\hbar^2|\Omega_{\mathrm{Rabi}}(\mathbf{r})|^2=\tfrac{1}{2}d_{\mathrm{rad}}^2\sum_i\sum_m|e_r(n,m,\nu_i,\mathbf{r})|^2. \quad (4.1)$$

The radial component of the sth TM mode of the atom located outside the microsphere, which is of interest to us, can easily be found from expression (2.3):

$$e_r(n,m,\nu,\mathbf{r})=-\frac{in(n+1)}{kr}[\alpha_{\mathrm{TM},n}^{(1)}h_n^{(1)}(kr)+\alpha_{\mathrm{TM},n}^{(2)}h_n^{(2)}(\mathrm{kr})]Y_{nm}(\vartheta,\varphi). \quad (4.2)$$

Note that $e_r(n,m,\nu)$ is related to the radial quantum number ν by the relation

$$k(\nu)=\frac{\omega_s}{c}=\frac{\omega(n,m,\nu)}{c}.$$

Summing the square of the absolute value of Eq. (4.2) with respect to the azimuthal quantum number m by means of the well-known relation

$$\sum_m|Y_{nm}|^2=\frac{2n+1}{4\pi}, \quad (4.3)$$

we get the following expression for the Rabi frequency:

$$\hbar^2|\Omega_{\mathrm{Rabi}}(\mathbf{r})|^2=\tfrac{1}{2}d_{\mathrm{rad}}^2E_{\mathrm{rad,TM}}^2,$$

$$E_{\mathrm{rad,TM}}^2=n(n+1)(2n+1)\sum_\nu\frac{2k(\nu)\hbar c}{\Lambda r^2}|j_n(k(\nu)r)-q_nh_n^{(1)}(k(\nu)r)|^2. \quad (4.4)$$

Using elementary relations, expression (4.4) can easily be reduced to the form

$$E_{\mathrm{rad,TM}}^2=n(n+1)(2n+1)\sum_\nu\frac{2k(\nu)\hbar c}{\Lambda r^2}[j_n(k(\nu)r)^2-\mathrm{Re}(q_nh_n^{(1)}(k(\nu)r)^2)]. \quad (4.5)$$

Replacing with the help of Eq. (2.12) the summation over radial quantum number ν by integration over frequencies in the frequency band $2\Delta\omega$ ($\Delta\omega\gg\Gamma_{\mathrm{res}}$) and extending the limits of integration in the second term of Eq. (4.5) to the interval $-\infty$, $+\infty$, we get the final expression for the mean square of the vacuum electric field:

$$E_{\mathrm{rad,TM}}^2=n(n+1)(2n+1)\frac{\pi\hbar\Gamma_{\mathrm{res}}}{2r^3}\left[Y_{n+1/2}^2(k_{\mathrm{res}}r)+J_{n+1/2}^2(k_{\mathrm{res}}r)\left(\frac{4\Delta\omega}{\pi\Gamma_{\mathrm{res}}}-1\right)\right], \quad (4.6)$$

where J_n and Y_n are the Bessel functions of the first and second kind, respectively [27], and $k_{\mathrm{res}}=\omega_{\mathrm{res}}/c$.

For long-lived modes, n is large and the term with J_n^2 is small compared with the term with Y_n^2. On the other hand, the terms proportional to $\Delta\omega J_n^2$ are specific to vacuum in the absence of the microsphere and must be subjected to a renormalization procedure, i.e., omitted. As a result, the expression for the vacuum field at the point r will assume the form

$$E_{\mathrm{rad,TM}}^2=n(n+1)(2n+1)\frac{\pi\hbar\Gamma_{\mathrm{res}}}{2r^3}[Y_{n+1/2}^2(k_{\mathrm{res}}r)]. \quad (4.7)$$

Note that expression (4.7) is proportional to the resonance width Γ_{res} of the microsphere. This is due to the fact that in the case under consideration the atom is located outside of the microsphere and can only get excited by virtue of the leakage of the vacuum energy from the microsphere.

In addition to the origination of the Rabi frequency, the dielectric microsphere is also responsible for a purely quasistatic shift of the atomic transition frequency. In our case, the quasistatic frequency shift is defined by the expression [18]

$$\omega_A^2=\omega_0^2-\delta\omega_0^2,$$
$$\delta\omega_0^2=\tfrac{3}{2}\omega_0\gamma_0\frac{a(\varepsilon-1)}{k_0^3r^4}\sum_{n=1}^{\infty}\frac{n(n+1)^2}{(\varepsilon+1)n+1}\left(\frac{a}{r}\right)^{2n}. \quad (4.8)$$

If the atom is very close to the microsphere, expression (4.8) is simplified:

$$\delta\omega_0^2=\frac{3}{8}\frac{\varepsilon-1}{\varepsilon+1}\frac{\gamma_0\omega_0}{[k_0(r-a)]^3}. \quad (4.9)$$

In expression (4.8), ω_0 stands for the atomic transition frequency in the absence of the microsphere,

$$\gamma_0=\frac{4d^2\omega_0^3}{3c^3\hbar} \quad (4.10)$$

is the linewidth in the absence of the microsphere, and $k_0=\omega_0/c$.

B. Tangential dipole moment orientation

Now let us consider the case of a tangentially oriented dipole. In that case, the dipole interacts with both TM and TE modes. This case can be analyzed in exactly the same way as the case of radial orientation.

For the Rabi frequency, we have the expression

$$\hbar^2|\Omega_{\mathrm{Rabi}}(\mathbf{r})|^2=\tfrac{1}{2}d_{\mathrm{tan}}^2E_{\mathrm{tan}}^2,$$
$$E_{\mathrm{tan}}^2=\sum_m\sum_j|e_{\mathrm{tan}}(n,m,\nu_j,\mathbf{r})|^2. \quad (4.11)$$

Note that as the position of the TM and TE resonances are determined (approximately) by the different expressions [see Eqs. (2.18) and (2.19)], interaction at a single frequency can take place either with a TM or with a TE mode. Therefore, when calculating the Rabi frequency, consideration should only be given for the electric fields of the corresponding mode.

The tangential component (we take it that this is the θ component) of the electric field outside of the microsphere has the form

$$e_{\tan}(n,m,\nu,\mathbf{r})=(e_{\mathrm{TM}})_{\tan}$$
$$=-\frac{i}{k}\frac{\partial}{r\partial r}r[\alpha^{(1)}_{\mathrm{TM},n}h^{(1)}_n(kr)$$
$$+\alpha^{(2)}_{\mathrm{TM},n}h^{(2)}_n(kr)]\frac{\partial Y_{nm}(\vartheta,\varphi)}{\partial\theta} \quad (4.12)$$

for the TM resonance and the form

$$e_{\tan}(n,m,\nu)=(e_{\mathrm{TE}})_{\tan}$$
$$=-[\alpha^{(1)}_{\mathrm{TE},n}h^{(1)}_n(kr)$$
$$+\alpha^{(2)}_{\mathrm{TE},n}h^{(2)}_n(\mathrm{kr})]\frac{mY_{\mathrm{nm}}(\vartheta,\varphi)}{\sin\theta} \quad (4.13)$$

for the TE resonance. Note that $e_{\tan}(n,m,\nu)$ is related to ν by the relation $k=\omega_s/c=\omega(n,m,\nu)/c$. Summing the squares of Eqs. (4.12) and (4.13) with respect to the azimuthal quantum number m and using the formulas

$$\frac{1}{\sin^2\theta}\sum_m m^2Y_{nm}Y^*_{nm}=\frac{n(n+1)(2n+1)}{8\pi}, \quad (4.14)$$

$$\sum_m \frac{\partial Y_{nm}}{\partial\theta}\frac{\partial Y^*_{nm}}{\partial\theta}=\frac{n(n+1)(2n+1)}{8\pi}, \quad (4.15)$$

we obtain, after averaging over frequencies in the interval $2\Delta\omega$ ($\Delta\omega\gg\Gamma_{\mathrm{res}}$) and renormalizing, the final expression for the effective tangential vacuum field.

In the case of TE resonance, we have the expression

$$E^2_{\tan,\mathrm{TE}}=(n+1/2)k^2_{\mathrm{res}}\frac{\pi\hbar\Gamma_{\mathrm{res}}}{2r}Y^2_{n+1/2}(k_{\mathrm{res}}r) \quad (4.16)$$

and in that of TM resonance, the expression

$$E^2_{\tan,\mathrm{TM}}=(n+1/2)\frac{\pi\hbar\Gamma_{\mathrm{res}}}{2r^3}[(n+1)Y_{n+1/2}(k_{\mathrm{res}}r)$$
$$-k_{\mathrm{res}}rY_{n+3/2}(k_{\mathrm{res}}r)]^2. \quad (4.17)$$

As in the radial case, the vacuum field given by Eqs. (4.16) and (4.17) is proportional to the linewidth of the microsphere and vanishes as it is reduced.

In addition to the origination of the Rabi frequency, the dielectric microsphere is also responsible for a purely quasistatic shift of the atomic transition frequency. In our case, the quasistatic frequency shift is defined by the expression [18]

$$\omega^2_A=\omega^2_0-\delta\omega^2_0,$$
$$\delta\omega^2_0=\tfrac{3}{4}\omega_0\gamma_0\frac{\varepsilon-1}{(k_0r)^3}\sum_{n=1}^{\infty}\frac{n^2(n+1)}{(\varepsilon+1)n+1}\left(\frac{a}{r}\right)^{2n}. \quad (4.18)$$

If the atom is very close to the surface, expression (4.18) is simplified:

$$\delta\omega^2_0=\frac{3}{16}\frac{\varepsilon-1}{\varepsilon+1}\frac{\gamma_0\omega_0}{[k_0(r-a)]^3}. \quad (4.19)$$

V. VACUUM FIELD AND RABI FREQUENCY IN THE CASE OF AN ATOM LOCATED INSIDE THE MICROSPHERE

By and large, the case of an atom located inside a dielectric microsphere can be considered in absolutely the same way as above. But in that case, account should be taken of the local field factor f causing both a change in the matrix elements

$$V_i\Rightarrow fV_i \quad (5.1)$$

and a change in the quasistatic frequency shift

$$\delta\omega^2_A\Rightarrow f^2\delta\omega^2_A. \quad (5.2)$$

As usual, we will take the local field factor to be given by [40]

$$f=\frac{3\varepsilon}{2\varepsilon+1}. \quad (5.3)$$

What is more, owing to the interaction with the crystal lattice of the microsphere material, the transition frequency ω_0 may differ from that in free space. We take no account of this circumstance in the present work.

A. Radial dipole moment orientation

To find the Rabi frequency in the case where the atom is inside the microsphere, use should be made of expression (2.3) for the electric field:

$$e_{\mathrm{rad}}(n,m,\nu,\mathbf{r})=-\frac{in(n+1)}{\varepsilon kr}[\beta_{\mathrm{TM},n}j_n(k\sqrt{\varepsilon}r)]Y_{nm}(\vartheta,\varphi). \quad (5.4)$$

Making absolutely the same calculations as in the case of an atom outside the microsphere, we obtain the following expression for the vacuum field inside the microsphere:

$$E^2_{\mathrm{rad,TM}}=n(n+1)(2n+1)\frac{\pi\hbar\Gamma_{\mathrm{res}}}{2\varepsilon^2r^3}J^2_{n+1/2}(\sqrt{\varepsilon}k_{\mathrm{res}}r)$$
$$\times\left(\frac{Y_{n+1/2}(k_{\mathrm{res}}a)}{J_{n+1/2}(\sqrt{\varepsilon}k_{\mathrm{res}}a)}\right)^2. \quad (5.5)$$

Note that in contrast to the derivation of Eq. (4.7), no diverging expressions appear in deriving expression (5.5), and so no need arises in renormalization. This circumstance is due to the fact that the field inside the microsphere has in principle no analogs in free space. Comparison between expression (5.5) and expression (4.7) for the vacuum field outside of the microsphere shows that there is a discontinuity due to the boundary conditions on the surface of the microsphere. For the electric displacement vector, continuity remains. The continuity of the electric displacement vector is evidence of the correctness of the renormalization procedure carried out in the case of an atom located outside of the microsphere. Another important feature of expression (5.5) is the fact that the vacuum field does not decrease with the decreasing resonance width Γ_{res}. Accordingly for the Rabi frequency, we have

$$\hbar^2|\Omega_{\mathrm{Rabi}}(\mathbf{r})|^2=\tfrac{1}{2}f^2d_{\mathrm{rad}}^2E_{\mathrm{rad,TM}}^2. \tag{5.6}$$

In addition to the origination of the Rabi frequency, the dielectric microsphere is also responsible for a purely quasistatic shift of the atomic transition frequency. In our case, the quasistatic frequency shift is defined by the expression [17]

$$\omega_A^2=\omega_0^2+\delta\omega_0^2,$$
$$\delta\omega_0^2=\tfrac{3}{2}\omega_0\gamma_0\frac{\varepsilon-1}{k_1^3ar^2}\sum_{n=0}^{\infty}\frac{n^2(n+1)}{(\varepsilon+1)n+1}\left(\frac{r}{a}\right)^{2n}. \tag{5.7}$$

If the atom is very close to the microsphere, expression (5.7) is simplified:

$$\delta\omega_0^2=\frac{3}{8}\frac{\varepsilon-1}{\varepsilon+1}\frac{\gamma_0\omega_0}{[k_0\sqrt{\varepsilon}(a-r)]^3}. \tag{5.8}$$

In expression (5.8), ω_0 stands for the atomic transition frequency in the absence of the microsphere,

$$\gamma_0=\frac{4d^2\omega_0^3}{3c^3\hbar}\sqrt{\varepsilon}f^2 \tag{5.9}$$

is the linewidth in the absence of the microsphere, i.e., in the case of unbounded dielectric medium, and $k_0=\omega_0/c$.

B. Tangential dipole moment orientation

In that case, the dipole interacts with both TM and TE modes. This case can be examined in exactly the same way as the case of radial orientation.

The tangential component (we take it that this is the θ component) of the electric field outside of the microsphere has the form

$$e_{\tan}(n,m,\nu)=(e_{\mathrm{TM}})_{\tan}=-\frac{i}{k}\frac{\partial}{r\partial r}r[\beta_{\mathrm{TM},n}j_n(k_1r)]\frac{\partial Y_{nm}(\vartheta,\varphi)}{\partial\theta} \tag{5.10}$$

for the TM resonance and the form

$$e_{\tan}(n,m,\nu)=(e_{\mathrm{TE}})_{\tan}=-[\beta_{\mathrm{TE},n}j_n(k_1r)]\frac{mY_{nm}(\vartheta,\varphi)}{\sin\theta} \tag{5.11}$$

for the TE resonance. Note that $e_{\tan}(n,m,\nu)$ is related to ν by the relation $k=\omega_s/c=\omega(n,m,\nu)/c$.

Summing the squares of Eqs. (5.10) and (5.11) with respect to the azimuthal quantum number m and using the formulas

$$\frac{1}{\sin^2\theta}\sum_m m^2Y_{nm}Y_{nm}^*=\frac{n(n+1)(2n+1)}{8\pi},$$
$$\sum_m\frac{\partial Y_{nm}}{\partial\theta}\frac{\partial Y_{nm}^*}{\partial\theta}=\frac{n(n+1)(2n+1)}{8\pi}, \tag{5.12}$$

we obtain, after averaging over frequencies, the final expression for the effective tangential vacuum field.

In the case of TE resonance, we have the expression

$$E_{\tan,\mathrm{TE}}^2=(n+1/2)k_{\mathrm{res}}^2\frac{\pi\hbar\Gamma_{\mathrm{res}}}{2r}\frac{J_{n+1/2}^2(\sqrt{\varepsilon}k_{\mathrm{res}}r)}{J_{n+1/2}^2(\sqrt{\varepsilon}k_{\mathrm{res}}a)}Y_{n+1/2}^2(k_{\mathrm{res}}a) \tag{5.13}$$

and in that of TM resonance, the expression

$$E_{\tan,\mathrm{TM}}^2=(n+1/2)\frac{\pi\hbar\Gamma_{\mathrm{res}}}{2r^3}\times\frac{[(n+1)J_{n+1/2}(k_{\mathrm{res}}r)-k_{\mathrm{res}}rJ_{n+3/2}(k_{\mathrm{res}}r)]^2}{[(n+1)J_{n+1/2}(k_{\mathrm{res}}a)-k_{\mathrm{res}}aJ_{n+3/2}(k_{\mathrm{res}}a)]^2}\times[(n+1)Y_{n+1/2}(k_{\mathrm{res}}a)-k_{\mathrm{res}}aY_{n+3/2}(k_{\mathrm{res}}a)]^2. \tag{5.14}$$

Note that the tangential vacuum field components suffer no discontinuity on the surface of the microsphere, which points to the correctness of the renormalization procedure in the preceding section. Another important feature of expressions (5.13) and (5.14) compared to the case of an atom outside of the microsphere is that the vacuum field does not decrease with the decreasing resonance width Γ_{res}. Another specific feature of the tangential case is the fact that the electrostatic frequency shift is half that in the case of radial orientation:

$$\omega_A^2=\omega_0^2+\delta\omega_0^2,$$
$$\delta\omega_0^2=\tfrac{3}{4}\omega_0\gamma_0\frac{\varepsilon-1}{k_1^3ar^2}\sum_{n=0}^{\infty}\frac{n(n+1)^2}{(\varepsilon+1)n+1}\left(\frac{r}{a}\right)^{2n}. \tag{5.15}$$

If the atom is close to the surface of the microsphere, expression (5.15) is simplified:

$$\delta\omega_0^2=\frac{3}{16}\frac{\varepsilon-1}{\varepsilon+1}\frac{\gamma_0\omega_0}{[k_0\sqrt{\varepsilon}(a-r)]^3}. \tag{5.16}$$

In expressions (5.15) and (5.16), γ_0 is the linewidth in the absence of the microsphere (5.9), i.e., in the case of unbounded dielectric medium, and $k_0=\omega_0/c$.

VI. NUMERICAL EXAMPLES AND PLOTS

The results of Sec. III, together with the expressions for the Rabi frequency in terms of the appropriate vacuum fields and quasistatic frequency shifts, enable one to easily obtain any characteristics of the system atom plus microsphere in the case of resonance interaction.

Figure 5 shows the square of the vacuum field strength as a function of the position of the atom for various atomic dipole orientations in the case of both outside and inside atom. It can be seen from this figure that in the case of tangential dipole orientation and TM resonance, the vacuum field reaches its maximum on the surface of the microsphere, while for other types of resonance, the maximum vacuum field is inside the microsphere and is two times as high as on the surface in the case of TE resonance and 1.5 times as high as that in the case of TM resonance.

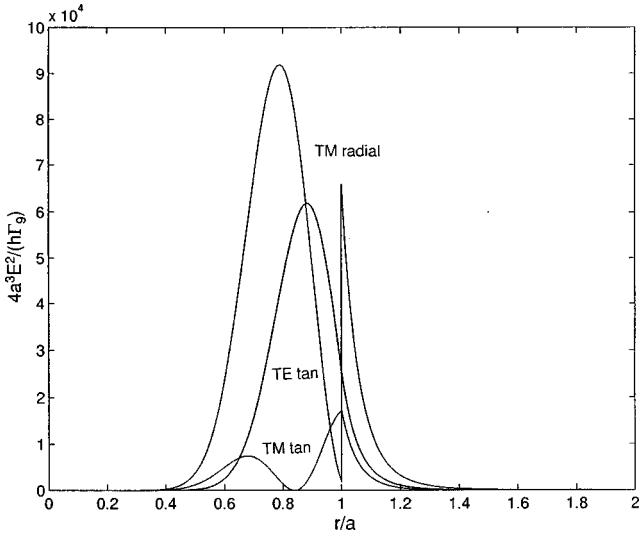

FIG. 5. Squared vacuum field strength as a function of the position of the atom in the case of radial dipole moment orientation (TM resonance with $n=9$, $ka=5.5487$) and tangential dipole moment orientation (TM resonance with $n=9$, $ka=5.5487$, and TE resonance with $n=10$ and $ka=5.619$).

For the modes with a higher quality factor (large n), the maxima inside the microsphere come closer to the surface of the microsphere and grow higher, which means that the effective volume of the mode is decreased.

Shown in Fig. 6 are the real and imaginary parts of the solutions of dispersion equation (3.23) with the parameters specially chosen such that at certain points in space there can occur exact resonance, i.e., the coincidence of complex solutions of Eq. (3.23). In the vicinity of the atom outside the microsphere, these curves coincide with those obtained in [22,24]. In these figures, one can clearly see the characteristic alternating regions of different frequency shifts or varying linewidths.

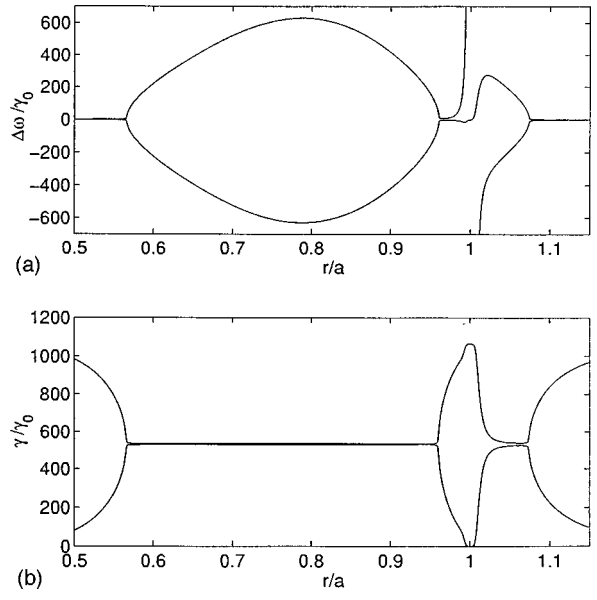

FIG. 6. (a) Frequency splitting and (b) radiative linewidths as a function of the position of the atom relative to the surface of the microsphere with due regard for the local field factor f [radial orientation of the dipole moment, TM(1,9,9) resonance $ka=5.5487$].

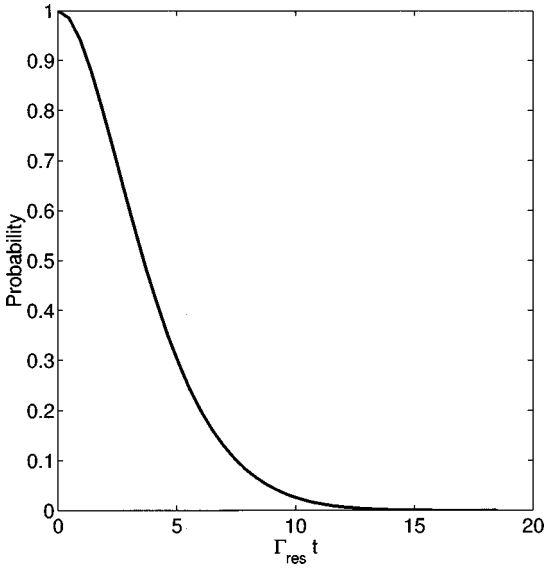

FIG. 7. Time dependence of the probability of the atom being in an excited state. The Weisskopf-Wigner regime (exponential decay) [$r/a=1.25$, $\omega_0/\gamma_0=10^8$, radial orientation of the dipole, TM(1,12,12) (a whispering gallery mode), $(ka)_{\rm res}=6.924\,298$, resonance case $\omega_A=\omega_{\rm res}$, initially excited atom].

Figures 7 and 8 show the temporal dynamics of the excited state of the atom and emitted photon spectrum in the case of weak interaction (the Weisskopf-Wigner case). In accordance with the results of Sec. III, under stronger interaction conditions the Weisskopf-Wigner regime is replaced by the vacuum Rabi-splitting regime (Figs. 9 and 10). One can see in Fig. 9 deep (down to zero) Rabi oscillations of the atomic excitation, and in Fig. 10, a doublet emitted photon spectrum.

Under strong interaction conditions wherein the atomic transition frequency differs from the resonance one, the Rabi

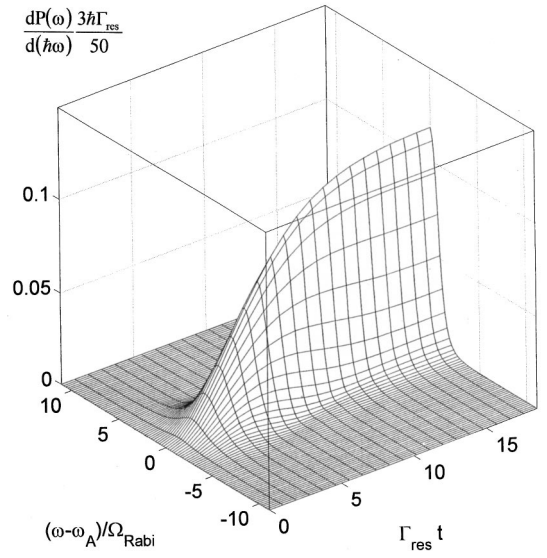

FIG. 8. Time dependence of the photon spectrum. The Weisskopf-Wigner regime (exponential decay) [$r/a=1.25$, $\omega_0/\gamma_0=10^8$, radial orientation of the dipole, TM(1,12,12) (a whispering gallery mode), $(ka)_{\rm res}=6.924\,298$, resonance case $\omega_A=\omega_{\rm res}$, initially excited atom].

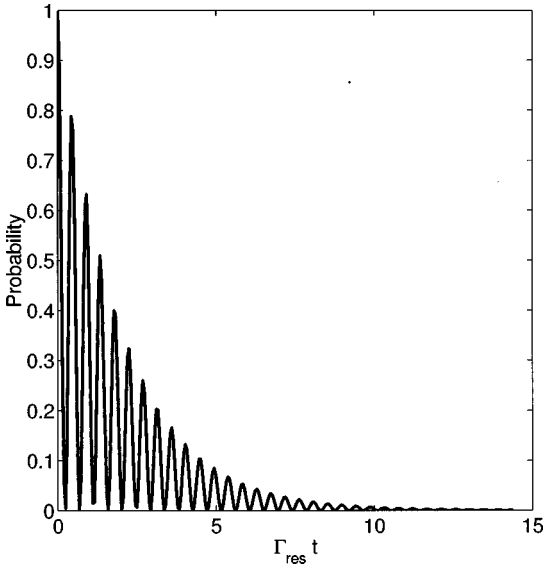

FIG. 9. Time dependence of the probability of the atom being in an excited state. The Rabi splitting regime [$r/a=0.8$, $\omega_0/\gamma_0=5\times10^7$, radial orientation of the dipole, TM(1,12,12) (a whispering gallery mode), $(ka)_{\rm res}=6.924\,298$, resonance case $\omega_A=\omega_{\rm res}$, initially excited atom].

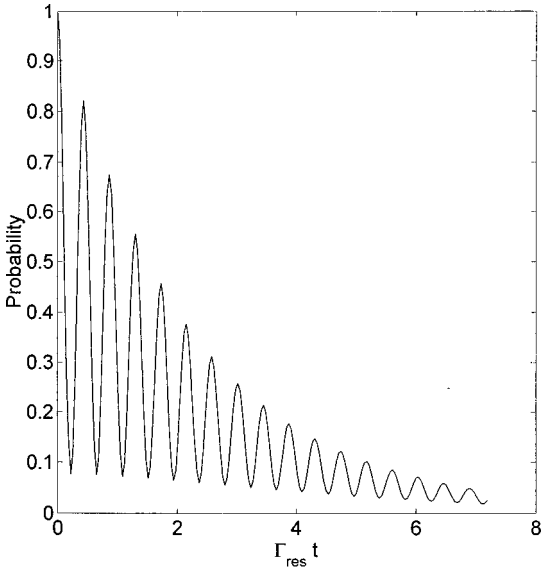

FIG. 11. Time dependence of the probability of the atom being in an excited state. The Rabi splitting regime [$r/a=0.8$, $\omega_0/\gamma_0=5\times10^7$, radial orientation of the dipole, TM(1,12,12) (a whispering gallery mode), $(ka)_{\rm res}=6.924\,298$, nonresonance case $\omega_A=\omega_{\rm res}+4\Gamma_{\rm res}$, initially excited atom].

oscillations become shallower (Fig. 11) and the doublet structure of the emitted photon spectrum becomes asymmetric (Fig. 12).

Let us consider now the case of an initially excited microsphere. In the case of sufficiently strong interaction (3.29) and optimal (as to phase) excitation (3.42) and (3.43), the dynamic atom-field relationships practically completely coincide with those in the case of an initially excited atom (Figs. 9–12). The weak interaction (Weisskopf-Wigner) regime is in that case specific, because the photon spectrum in the case of an initially excited microsphere always remains of doublet type (Figs. 13 and 14) in contrast to its singlet structure in the case of an initially excited atom (Figs. 7 and 8).

More interesting is the case of incomplete phase matching of the excitation line. In that case, the probability amplitude of the atom being in an excited state is characterized by deep oscillations, but its maximum excitation probability is substantially less than unity and is defined by factor (3.46) (Fig. 15). As a result of incomplete excitation of the atom, the fluorescence spectrum has a triplet structure (Fig. 16).

Figure 17 shows the relationship between the fluorescence

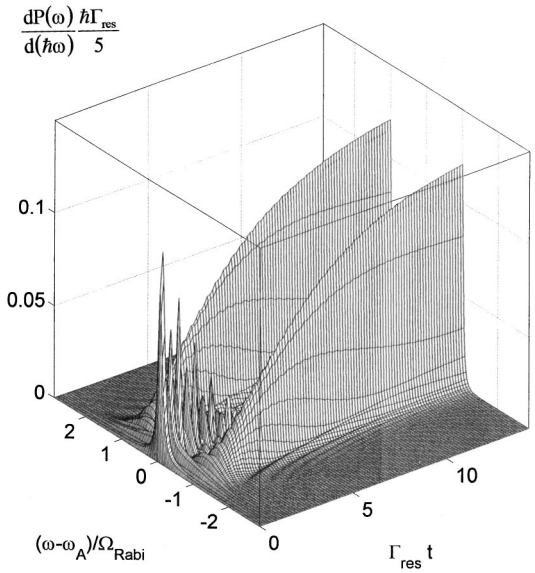

FIG. 10. Time dependence of the photon spectrum. The Rabi splitting regime [$r/a=0.8$, $\omega_0/\gamma_0=5\times10^7$, radial orientation of the dipole, TM(1,12,12) (a whispering gallery mode), $(ka)_{\rm res}=6.924\,298$, resonance case $\omega_A=\omega_{\rm res}$, initially excited atom].

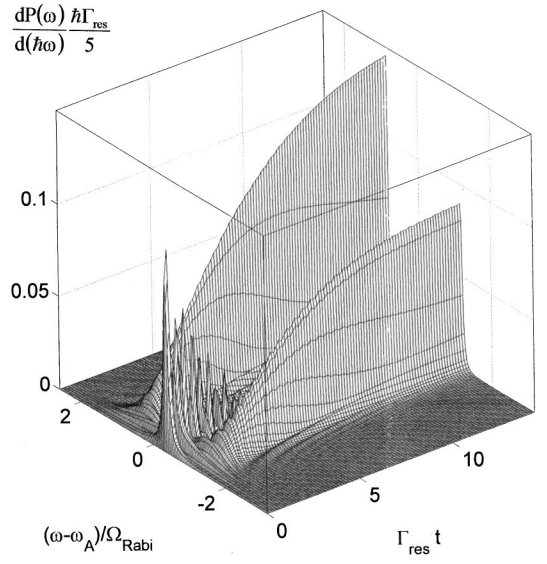

FIG. 12. Time dependence of the photon spectrum. The Rabi splitting regime [$r/a=0.8$, $\omega_0/\gamma_0=5\times10^7$, radial orientation of the dipole, TM(1,12,12) (a whispering gallery mode), $(ka)_{\rm res}=6.924\,298$, nonresonance case $\omega_A=\omega_{\rm res}+2\Gamma_{\rm res}$, initially excited atom].

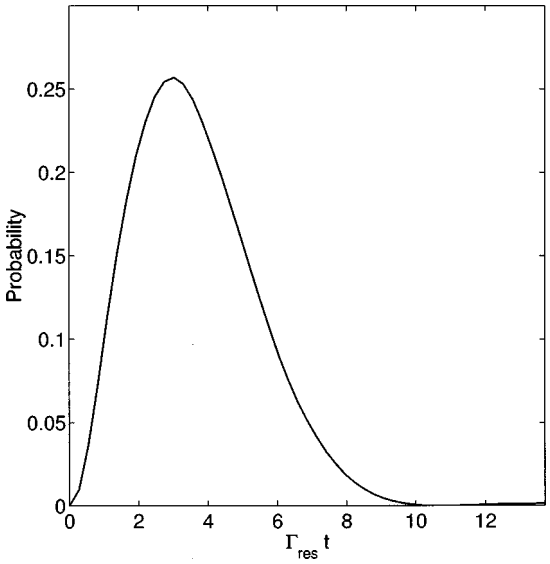

FIG. 13. Time dependence of the probability of the atom being in an excited state. The Weisskopf-Wigner regime (exponential decay) [$r/a=1.25$, $\omega_0/\gamma_0=10^8$, radial orientation of the dipole, TM(1,12,12) (a whispering gallery mode), $(ka)_{\rm res}=6.924\,298$, optimal excitation of the microsphere].

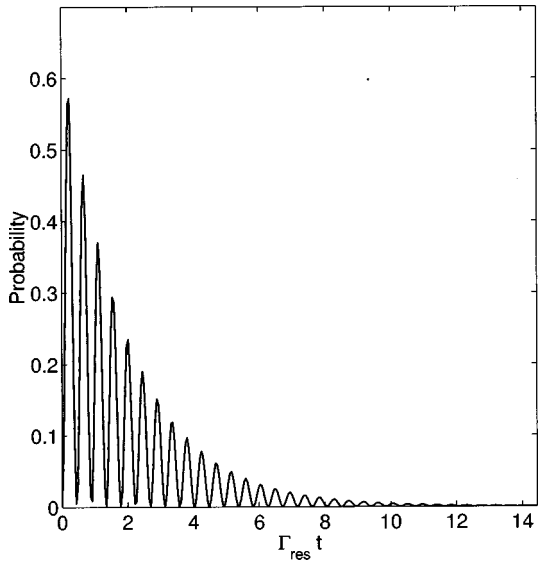

FIG. 15. Time dependence of the probability of the atom being in an excited state. The triplet splitting regime [$r/a=0.8$, $\omega_0/\gamma_0=5\times10^7$, radial orientation of the dipole, TM(1,12,12) (a whispering gallery mode), $(ka)_{\rm res}=6.924\,298$, resonance case $\omega_A=\omega_{\rm res}$, the microsphere is excited in accordance with Eq. (3.44), $\Gamma_\Psi/\Gamma_{\rm res}=0.25$].

spectrum and the degree of phase matching between the excitation line and the microsphere. It is clearly seen in the figure how the doublet structure (the solid line) which is typical of optimum matching (3.47) and (3.50) changes over to the triplet structure (the dotted line) specific to nonoptimal matching (3.54), and then to the singlet structure (the dashed line) in the case of phase antimatching (3.51) and (3.53). Note, the energetical profile of the excitation line is the same for all cases presented in Fig. 17.

VII. CONCLUSION

Thus, we have considered in the present work the interaction of a two-level atom with the continuum of modes modified by the presence of a dielectric microsphere in the frequency region corresponding to the occurrence of whispering gallery modes in the microsphere.

Subject to minimal assumptions, we have obtained on first principles simple expressions describing the spectral characteristics of the system and relaxation processes occurring therein. Our main assumption is that the atom predominantly

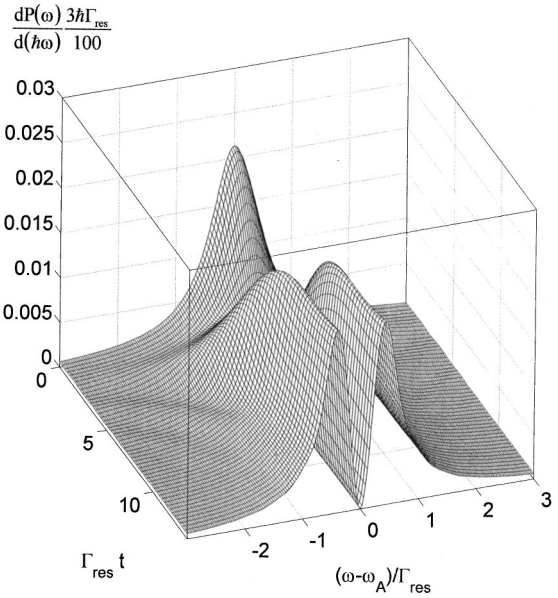

FIG. 14. Time dependence of the photon spectrum. The Weisskopf-Wigner regime (exponential decay) [$r/a=1.25$, $\omega_0/\gamma_0=10^8$, radial orientation of the dipole, TM(1,12,12) (a whispering gallery mode), $(ka)_{\rm res}=6.924\,298$, optimal excitation of the microsphere].

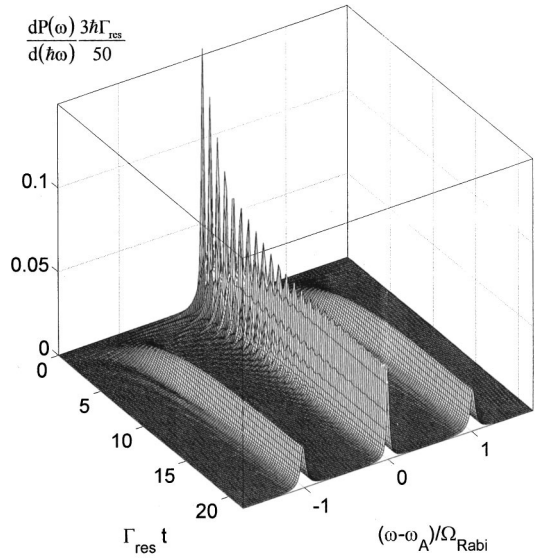

FIG. 16. Time dependence of the photon spectrum. The triplet splitting regime [$r/a=0.8$, $\omega_0/\gamma_0=5\times10^7$, radial orientation of the dipole, TM(1,12,12) (a whispering gallery mode), $(ka)_{\rm res}=6.924\,298$, resonance case $\omega_A=\omega_{\rm res}$, the microsphere is excited in accordance with Eq. (3.44), $\Gamma_\Psi/\Gamma_{\rm res}=0.25$].

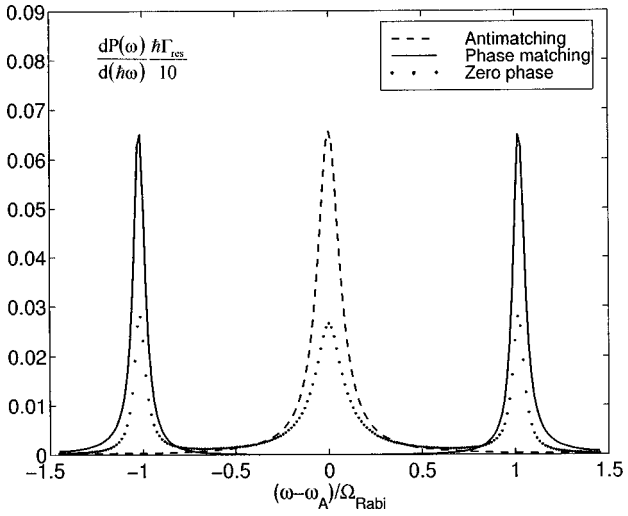

FIG. 17. Fluorescence spectrum as a function of the microsphere excitation method $(\omega)_A=\omega_{\rm res}$, $|\Omega_\Psi|=|\Omega_{\rm res}|$: (a) maximum possible concentration of the photon energy in the microsphere (3.50) (solid line); (b) minimum possible concentration of the photon energy in the microsphere (3.53) (dashed line); (c) intermediate case (3.54) (dotted line) [$r/a=0.8$, $\omega_0/\gamma_0=5\times10^7$, radial orientation of the dipole, TM(1,12,12) (a whispering gallery mode), $(ka)_{\rm res}=6.924\,298$].

interacts with continuum quantized modes falling within the profile of one of the whispering gallery mode, the criterion of which is the smallness of the Rabi frequency in comparison with the distance between the resonances of the microsphere. The weak interaction with the rest of the quantized modes (other frequencies, other n's) may effectively be accounted for by adding the appropriate imaginary part to the energy of the atom (the Breit-Wigner procedure [41]).

The main characteristics of the system (the dispersion equation, oscillation frequencies, and decay parameters) fully coincide with the corresponding characteristics found when analyzing the classical system [22].

When the atom is excited at the initial instant, a doublet structure is formed in the emitted photon spectrum, provided that interaction is strong enough.

If it is the microsphere that is excited at the initial instant, the emitted photon spectrum depends substantially on the excitation method. In the case of optimum excitation where the excitation linewidth is equal to the resonance linewidth, there takes place an effective excitation of the atom, followed by the formation of a Rabi doublet in the fluorescence spectrum. If excitation conditions deviate from the optimal ones, the spectrum becomes of triplet type. Where the deviation from the optimal excitation conditions is great, the atom practically remains unexcited, and the fluorescence spectrum is of singlet character.

A substantial proportion of the results obtained in Sec. III are of general character and can be applied to other cases of strong atom-cavity interaction.

ACKNOWLEDGMENTS

The authors thank the Russian Basic Research Foundation and the U.S. Department of Defense (through the intermediary of the University of Arizona) for their financial support of this work.

[1] V. B. Braginsky, M. L. Gorodetsky, and V. S. Ilchenko, Phys. Lett. A **137**, 393 (1989).
[2] S. Schiller and R. L. Byer, Opt. Lett. **16**, 1138 (1991).
[3] L. Collot, V. Lefevre, M. Brune, J.-M. Raimond, and S. Haroche, Europhys. Lett. **23**, 327 (1993).
[4] M. L. Gorodetsky, A. A. Savchenkov, and V. S. Ilchenko, Opt. Lett. **21**, 453 (1996).
[5] G. S. Dutta and G. S. Agarwal, Opt. Commun. **115**, 597 (1995).
[6] F. Bernadot, P. Nussenzveig, M. Brune, J.-M. Raimond, and S. Haroche, Europhys. Lett. **17**, 33 (1991).
[7] V. B. Braginsky and F. Y. Khalili, Zh. Eksp. Teor. Fiz. **78**, 1712 (1977) [Sov. Phys. JETP **46**, 705 (1977)].
[8] S. Haroche, M. Brune, and J.-M. Raimond, J. Phys. II **2**, 659 (1992).
[9] V. Sandoghdar, F. Treussart, J. Hare, V. Lefevre-Seguin, J.-M. Raimond, and S. Haroche, Phys. Rev. A **54**, R1777 (1996).
[10] J.-M. Raimond, in *Quantum Optics of Confined Systems*, edited by M. Ducloy and D. Bloch (Kluwer, Dordrecht, 1996), pp. 1–46.
[11] R. Feynman, Opt. News **11**, 11 (1985); Found Phys. **16**, 507 (1986).
[12] Q. A. Turchette, C. J. Hood, W. Lange, H. Mabucci, and H. J. Kimble, Phys. Rev. Lett. **75**, 4710 (1995).
[13] C. Monroe, D. M. Meekhof, B. E. King, W. M. Itano, and D. J. Wineland, Phys. Rev. Lett. **75**, 4714 (1995).
[14] P. Domokos, J.-M. Raimond, M. Brune, and S. Haroche, Phys. Rev. A **52**, 3554 (1995).
[15] H. Chew, P. J. McNulty, and M. Kerker, Phys. Rev. A **13**, 396 (1976).
[16] H. Chew, J. Chem. Phys. **87**, 1355 (1987).
[17] V. V. Klimov, M. Ducloy, and V. S. Letokhov, J. Mod. Opt. **43**, 549 (1996).
[18] V. V. Klimov, M. Ducloy, and V. S. Letokhov, J. Mod. Opt. **43**, 2251 (1996).
[19] F. V. Bunkin and A. N. Oraevsky, Izv. Vyssh. Uchebn. Zaved. Radiofiz. **2**, 181 (1959).
[20] G. Rempe, H. Walther, and N. Klein, Phys. Rev. Lett. **58**, 353 (1987).
[21] S. Haroche, in *Fundamental Systems in Quantum Optics* (Elsevier, Amsterdam, 1992).
[22] V. Klimov, M. Ducloy, and V. Letokhov, J. Mod. Opt. **44**, 1081 (1997).
[23] I. Takahashi and K. Ujihara, Phys. Rev. A **56**, 2299 (1997).
[24] V. V. Klimov, M. Ducloy, and V. S. Letokhov, Phys. Rev. A **56**, 2308 (1997); V. V. Klimov and V. S. Letokhov, Zh. Eksp. Teor. Fiz. **111**, 44 (1997) [JETP **84**, 24 (1997)].
[25] V. V. Klimov and V. S. Letokhov, JETP Lett. **68**, 124 (1998).
[26] A. S. Davydov, *Quantum Mechanics* (Nauka, Moscow, 1973) (in Russian).

[27] *Handbook of Mathematical Functions*, edited by M. Abramovitz and I. A. Stegun (U.S. GPO, Washington, DC, 1964).
[28] G. Mie, Ann. Phys. (Leipzig) **B25**, S377 (1908).
[29] R. Courant and D. Hilbert, *Methods of Mathematical Physics* (Gostekhizdat, Moscow, 1951), Vol. 1 (in Russian).
[30] L. A. Vainstein, *Electromagnetic Waves* (Radio i Sviaz, Moscow, 1988) (in Russian).
[31] H. M. Nussenzveig, *Diffraction Effects in Semiclassical Scattering* (Cambridge University Press, Cambridge, 1992).
[32] L. A. Vainstein, *Opened Resonators and Waveguides* (Sov. Radio, Moscow, 1966) (in Russian).
[33] D. P. Craig and T. Thirunamachandran, *Molecular Quantum Electrodynamics* (Academic, London, 1984).
[34] R. Loudon, *The Quantum Theory of Light* (Clarendon, Oxford, 1973).
[35] C. Cohen-Tannoudji and P. Avan, in *Atoms in Electromagnetic Fields* (World Scientific, Singapore, 1994), p. 328.
[36] O. Rice, Phys. Rev. **33**, 748 (1929).
[37] B. I. Stepanov, Zh. Eksp. Teor. Fiz. **15**, 435 (1945).
[38] V. Weisskopf and E. P. Wigner, Z. Phys. **63**, 54 (1930).
[39] B. R. Mollow, Phys. Rev. **188**, 1969 (1969).
[40] R. J. Glauber and M. Lewenstein, Phys. Rev. A **43**, 467 (1991).
[41] G. Breit and E. P. Wigner, Phys. Rev. **49**, 519 (1936); **49**, 642 (1936).